Simplified Powder Processing and Microstructural Control of Fe-based ODS Alloys

J. R. Rieken[1], I.E. Anderson[2], and M.J. Kramer[2]

[1]Materials Science and Engineering, Iowa State University, Ames, IA

[2]Division of Materials Sciences and Engineering, Ames Laboratory (USDOE), Ames, IA

"Fe-Based ODS Alloys: Role and Future Applications"

Fabrication, Microstructure Preservation & Mechanical Properties

University of California-San Diego: November 18th, 2010, San Diego, CA

Support from the Department of Energy-Office of Fossil Energy is gratefully acknowledged through Ames Laboratory contract no. DE-AC02-07CH11358

Future Generation Power Reactors

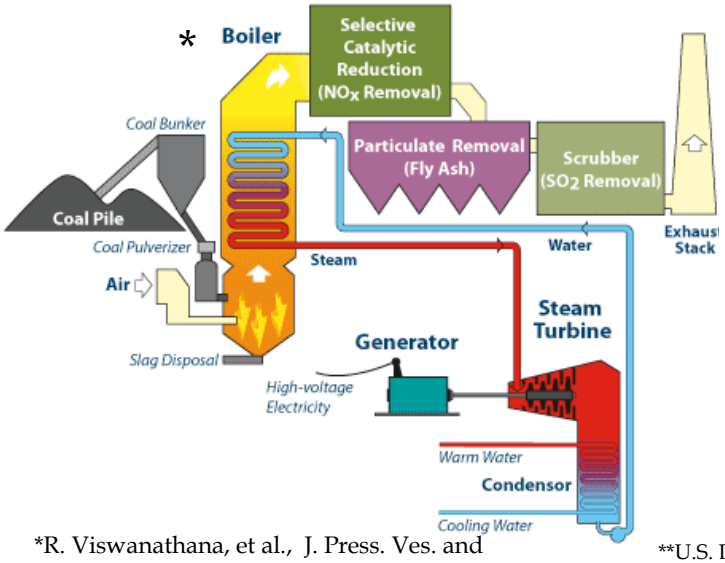

*R. Viswanathana, et al., J. Press. Ves. and Pip., 2006. **83**: p. 778-783.

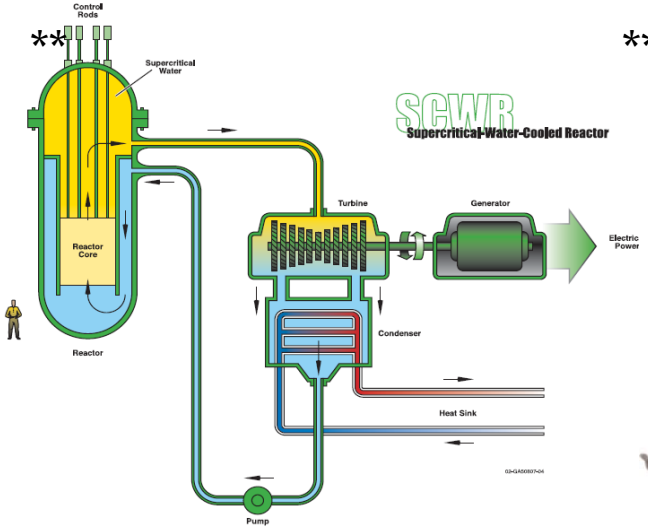

**U.S. DOE Nuclear Energy Research Advisory Committee, and Generation IV International Forum GIF, GIF-002-00 OECD Nuc. E. Agency, 2002: p. 1-90.

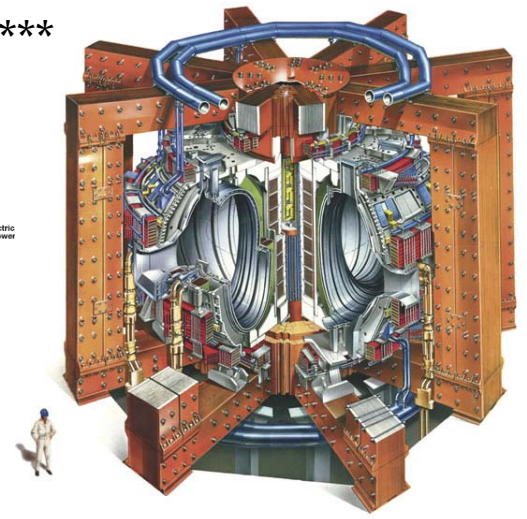

***ITER, *The ITER Device.* http://www.iter.org/a/index_nav_4.htm, 2009.

Material	Cost/kg (USD)	Notes
Ferritic Stainless Steel	~$2-5	446 Plate form
Austenitic Stainless Steel	~$3-7	316L Plate form
F/M Fe-9Cr steels	≤$5.50	Plate form
Ni-based	~$30-35	Inconel 718 Sheet (Special Metals), Inconel 617 (Special Metals)
Fe-based ODS	~$165, ~$345	MA956 Sheet (Special Metals), PM 2000 (Plansee)
V-4Cr-4Ti	~$200	Plate form (Average between 1994 and 1996 US fusion program large heats)
SiC_f/SiC_m composites	~$1000, ~$200	Chemical vapor infiltration, and Chemical vapor reaction

ODS Processing Cost!

J.T. Busby, J. Nuc. Mat., 2009. **392**: p. 304
K. Savolainen, J. Mononen, R. Ilola, and H. Hänninen, 2005, Helsinki University of Technology, Laboratory of Engineering Materials Publications.

S.J. Zinkle and N.M Ghoniem, Fusion Engineering and Design 2000. **51**(52): p. 55-71.
Special Metals Price Quote

Motivation

Mechanical Alloying:

- A high-energy mixing process that violently blends master alloy powders with nano-metric oxide powders into a supersaturated solid solution, during which complex folding, cold welding, and fracturing of the powders takes place in a high-energy mill
- **MA processing* can take numerous hours of milling time (t>40hr), which can lead to high levels of contamination from milling debris and gas environment**
- Hot deformation consolidation and recrystallization can lead to an anisotropic microstructure and directional mechanical properties

***This complex process can lead to an extremely high raw material cost, e.g., ~$340/kg for PM2000.** *J.T. Busby, J. Nuc. Mat., 2009. **392**: p. 304

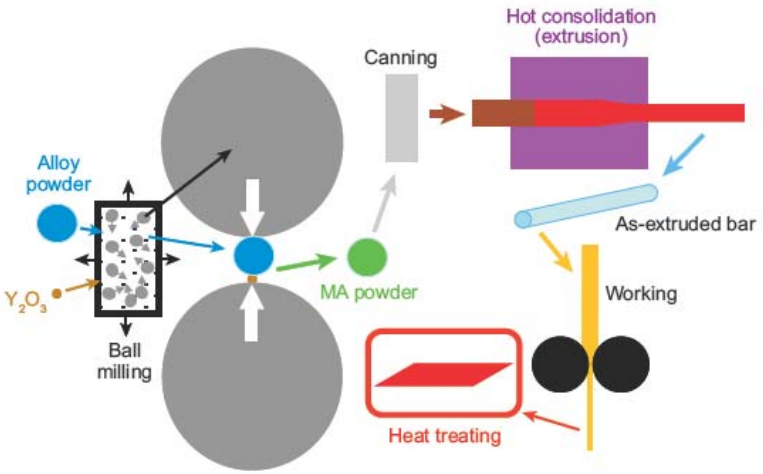

G.R. Odette, et al., Annu. Rev. Mater. Res., 2008. **38**: p. 471-503

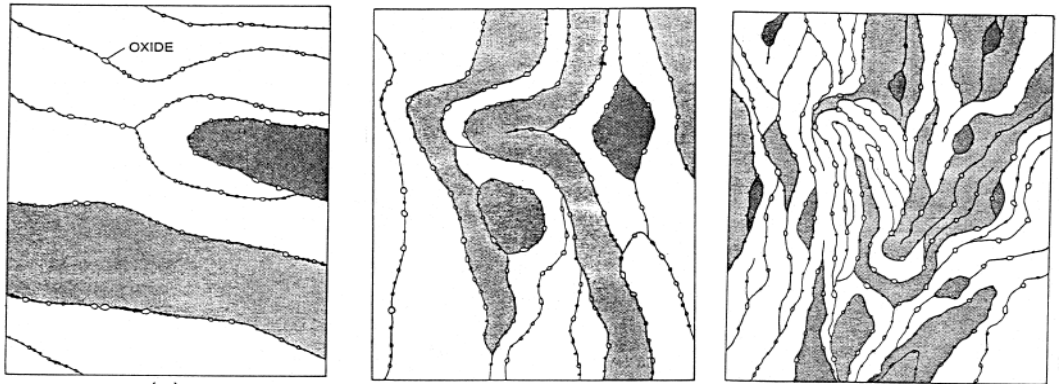

C. Suryanarayana, Prog. in Mat. Sci., 2001. **46**: p. 1-184

Processing Comparison

* **Mechanical Alloying**
  - Long milling times
  - Batch commercial process (~2000 kg)
  - Powder contamination (milling debris, C, O, N, Ar)
  - Anisotropic microstructure

** **Gas Atomization (RSP)**
  - Higher processing rates (10-100 kg/min)
  - Continuous processing capacity
  - Minimized contamination
  - Isotropic microstructure

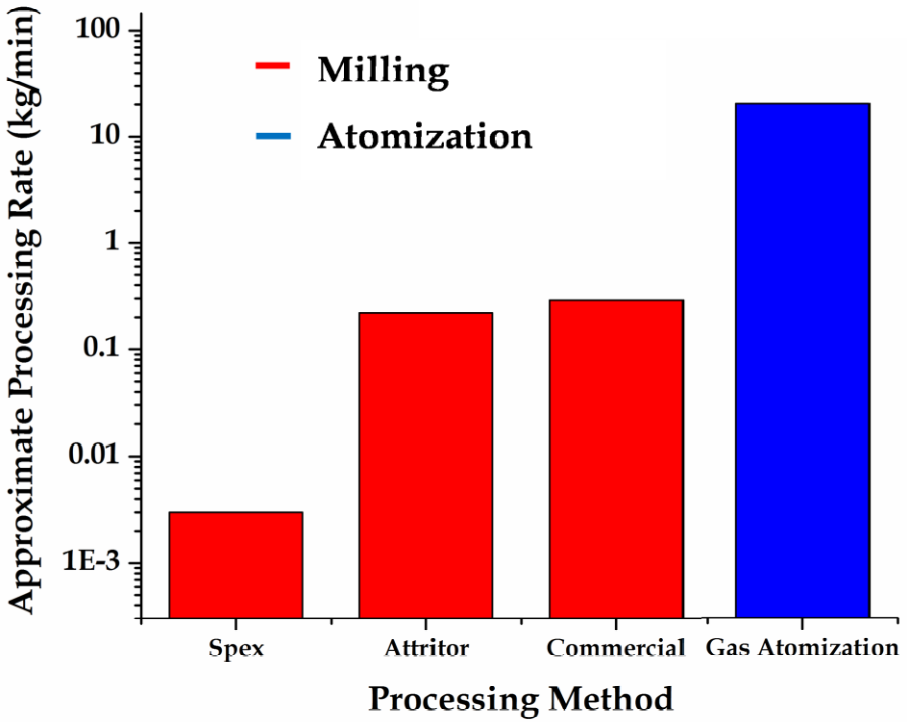

Increased powder processing rates, using gas atomization, could promote a significant reduction in raw material cost (~3-5X)

*C. Suryanarayana, ASM Handbook, Vo. 7, ASM International, Materials Park, OH, 1998, pp. 80-90.

**R.M. German, *Powder Metallurgy and Particulate Materials Processing*, 2005, MPIF, Princeton, NJ.

New Simplified Gas Atomization Process

1) Gas Atomization Reaction Synthesis (GARS)# – *in situ* alloying
   - Chemical reaction chamber
   - Oxide dispersion forming precursor powder
2) Hot Isostatically Pressed to Full Consolidation
   - Dispersoid phase formation
   - Equiaxed grain structure and isotropic mechanical properties
3) Thermal-Mechanical Treatment
   - Dislocation substructure formation (ultimate strengthening)**

**B.A. Wilcox, et al., in *Strength of Metals and Alloys*. 1967.

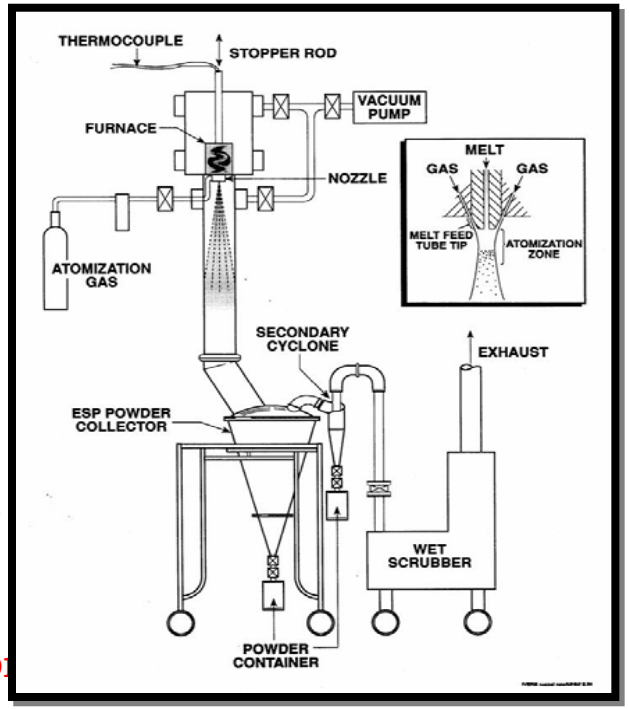

Eliminates inefficient mechanical alloying and directio deformation processing.

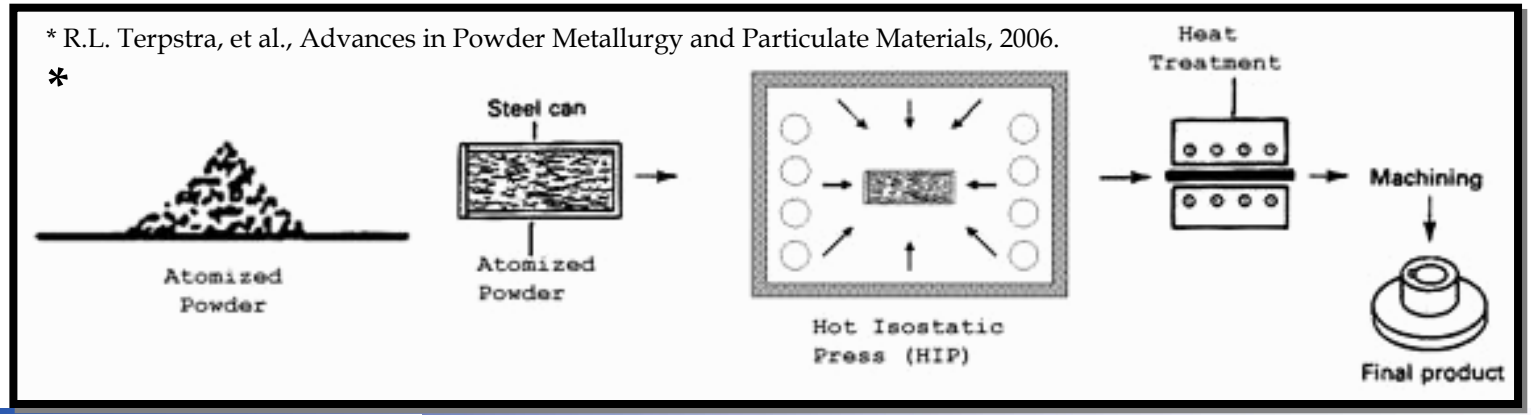

#I.E. Anderson, et al., *Gas atomization synthesis of refractory or intermetallic compounds and supersaturated solid solutions*, USPTO no. 5,368,657. 1994.

Chemical Reservoir – Alloy Design

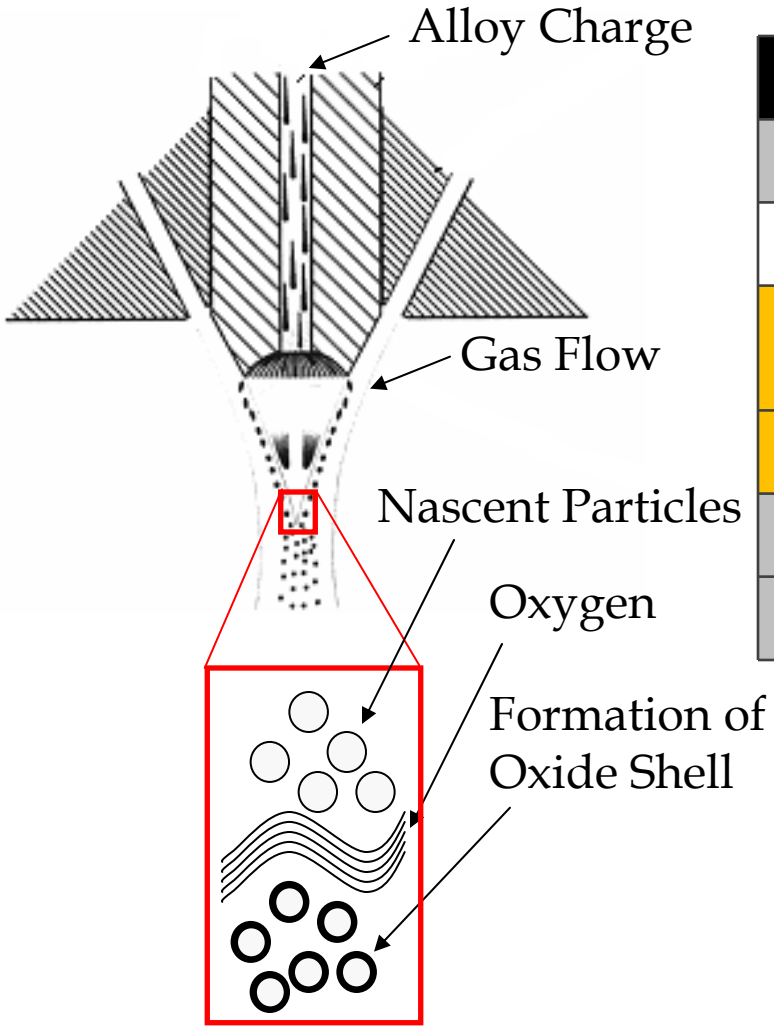

Element	Alloying Motivation	Approx. Conc. (at.%)
Chromium	Surface reactant and corrosion resistance	15.0-16.0
Yttrium	Highly stable nano-metric oxide dispersoid former	0.1-0.2
Titanium	Surface reactant, dispersoid stabilizer, and interstitial impurity scavenger	0.4-0.5
Hafnium	Dispersoid stabilizer and interstitial impurity scavenger	0.1-0.3
Tungsten	Solid solution and/or precipitate strengthener	1.0
Oxygen (rxn. gas)	Surface oxidant and nano-metric oxide dispersoid former	0.35-0.70

GARS Processing:

- **Rapid Solidification Process (solute trapping??)**
- **Reactive gas (Ar-O_2)**
- **In situ surface oxidation of the most kinetically favored oxide phase (metastable Cr-enriched oxide)**

Dispersoid Formation Mechanism

Oxygen Exchange Reaction

- Dissociation of the less stable prior particle boundary (PPB) oxide
- Oxygen diffusion away from PPBs
- Nano-metric Y-enriched oxide formation

- ***Full dissociation of PPB oxide will be necessary for ideal mechanical properties***

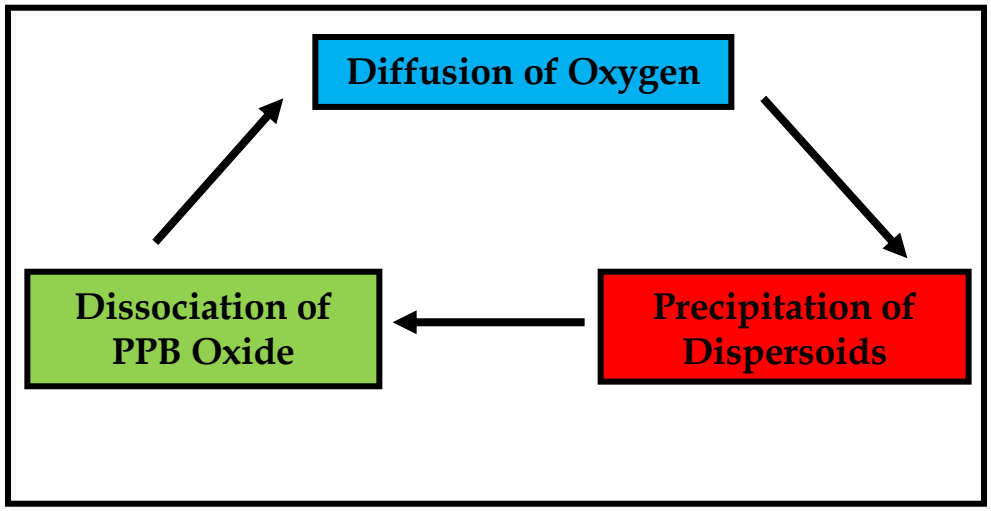

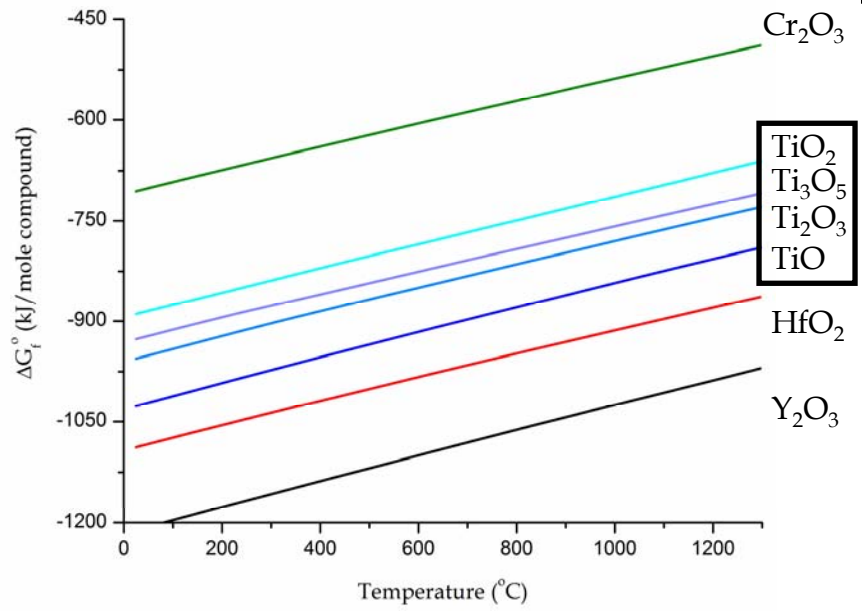

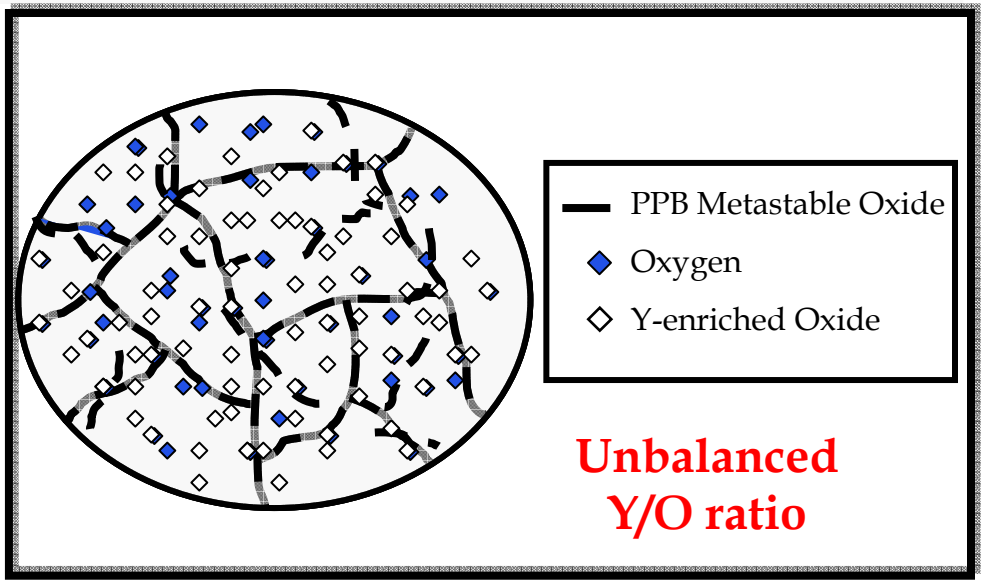

Sauert F., et al., Thermochemical Data of Pure Substances, 2nd Edition 1992.

CR-Alloy Composition and Experimental Parameters

Alloy		Fe (at.%)	Cr (at.%)	Hf (at.%)	Y (at.%)	O (at.%)	Rxn Gas (vol.%)	Rxn Gas Inlet
CR-156YHf	Nominal	Bal.	16.0	0.12	0.31	-	Ar-0.12O_2	HPGA Nozzle
CR-156YHf	Resulting	Bal.	15.84	0.11	0.18	0.38	Ar-0.12O_2	HPGA Nozzle

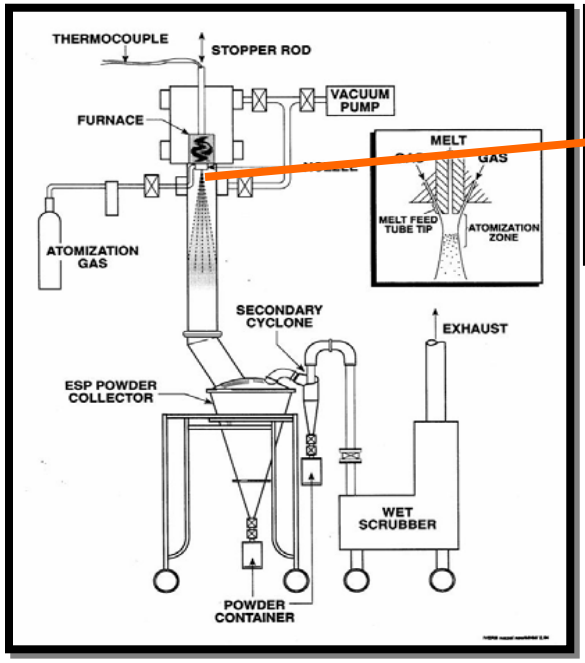

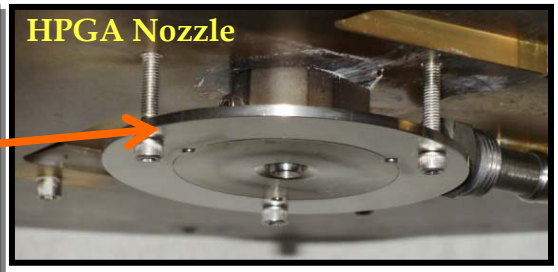

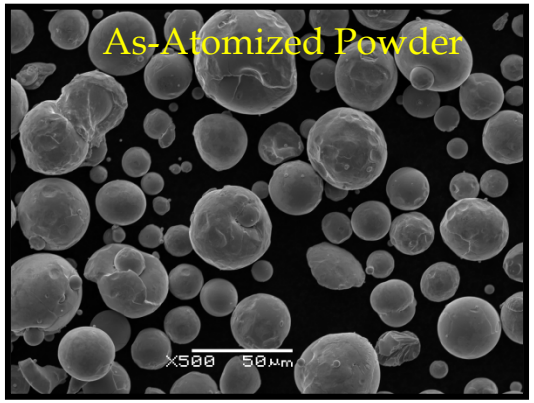

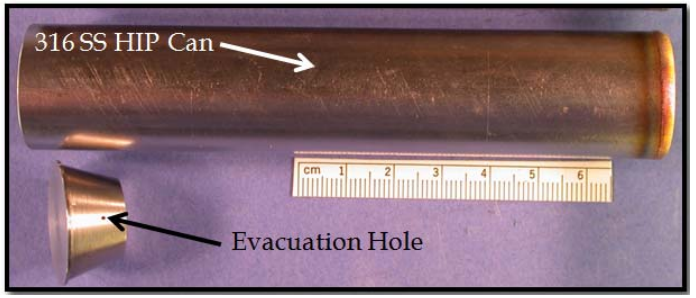

1) Size Classify Powders (<5, 5-20, 20-53µm)
2) Low temperature consolidation (700°C-200MPa-4hr)
3) Elevated temperature heat treatment (1200°C-2.5hr)
   *Predicted from internal oxidation experiments

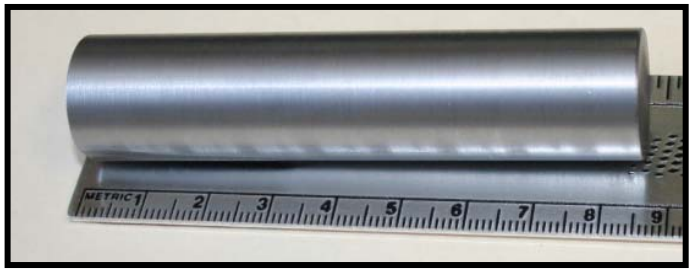

CR-156Y-Hf: Fe-15.84Cr-0.11Hf-0.18Y-0.38O at.%

Reactive Atomization Process Control

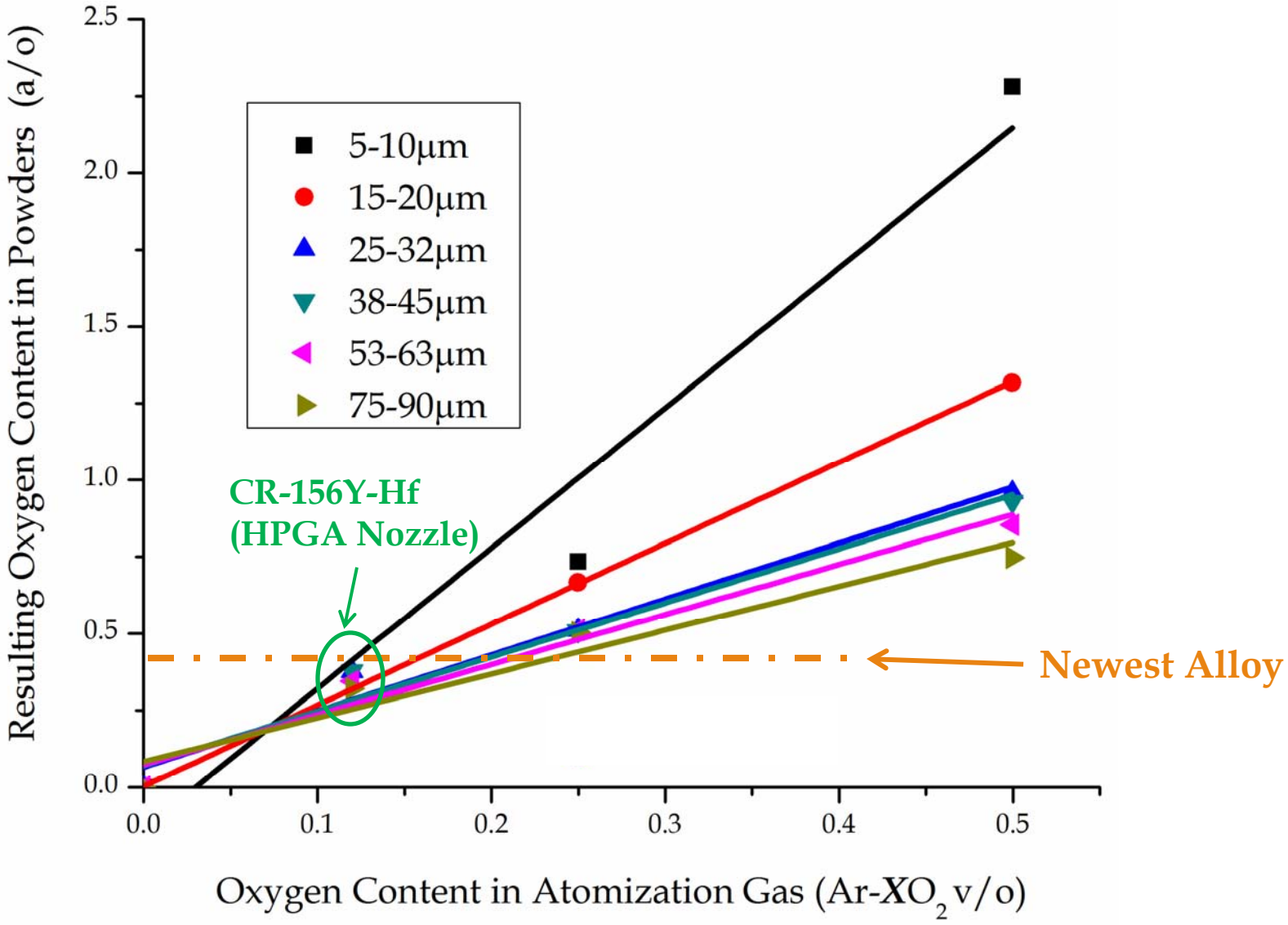

XRD Characterization of Phase Evolution

CR-156Y-Hf: Fe-15.84Cr-0.11Hf-0.18Y-0.38O at.%

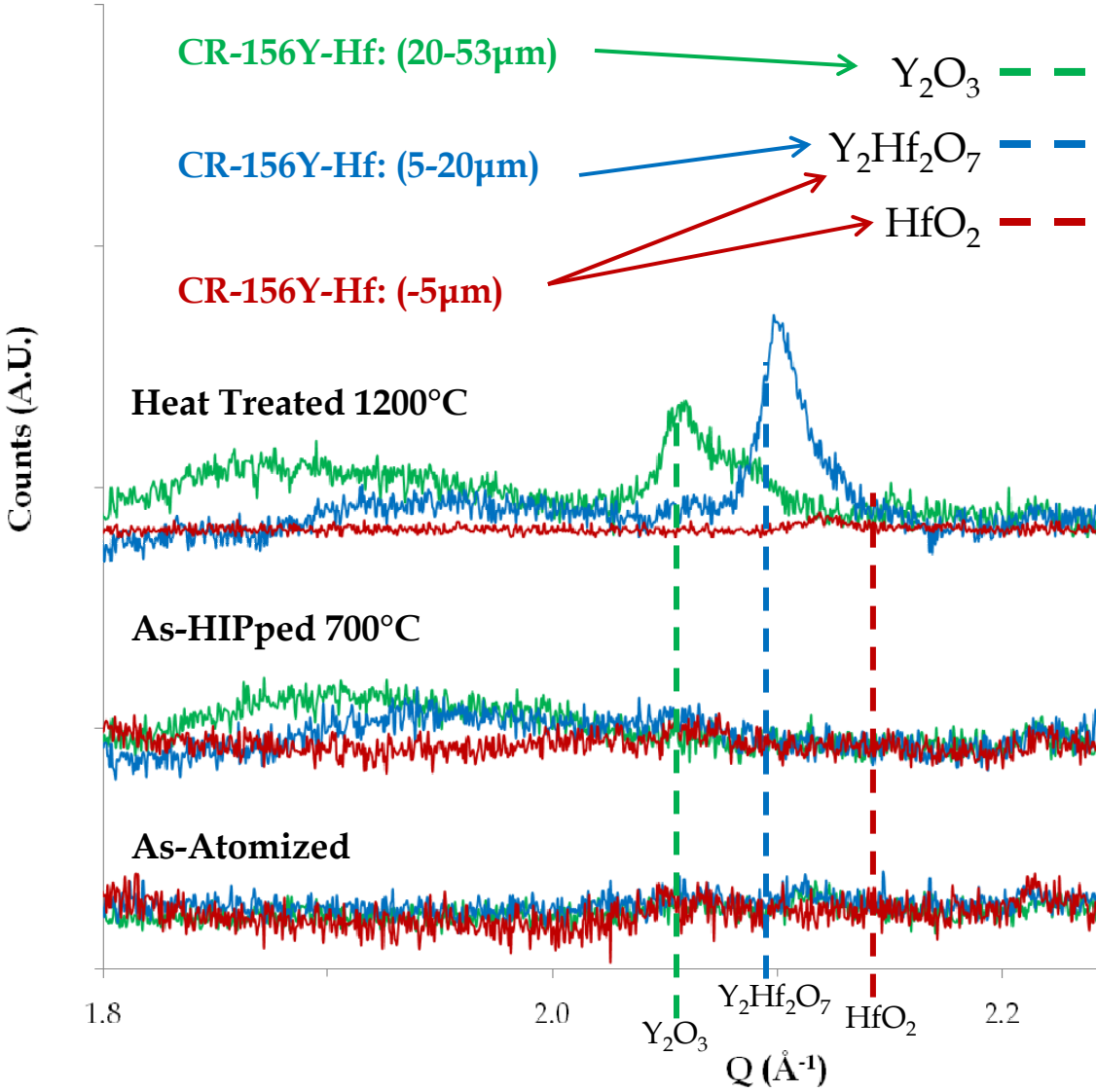

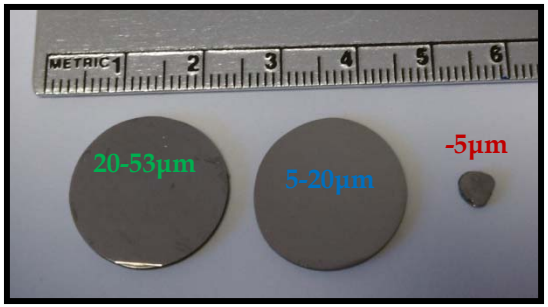

- Traditional XRD (Co-Kα)
- To be confirmed using HE-XRD

As-Atomized Microstructure

CR-156Y-Hf: Fe-15.84Cr-0.11Hf-0.18Y-0.38O at.%

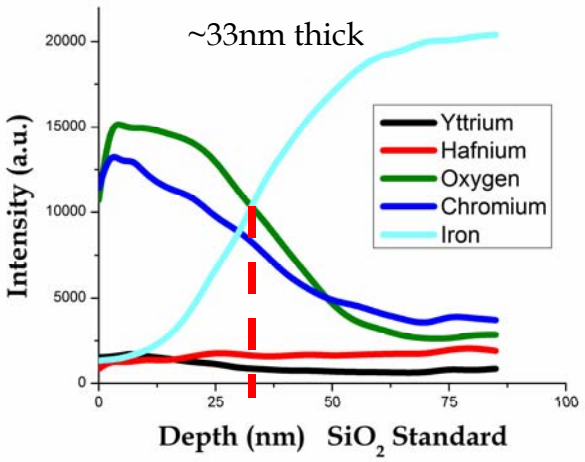

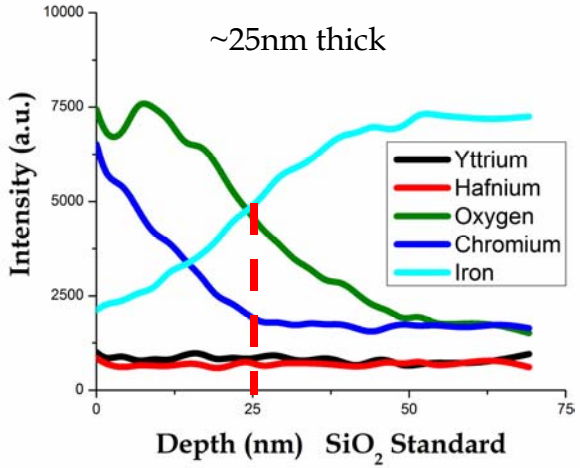

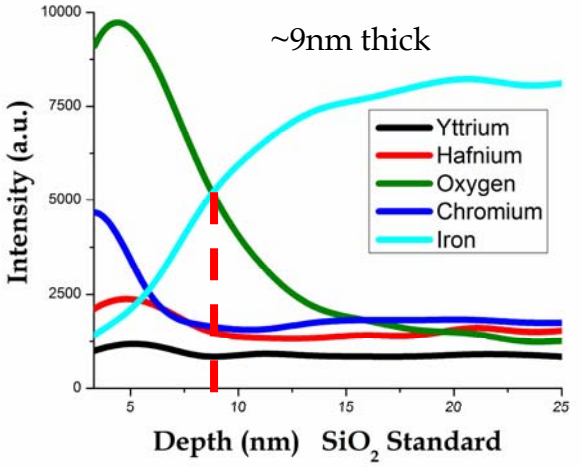

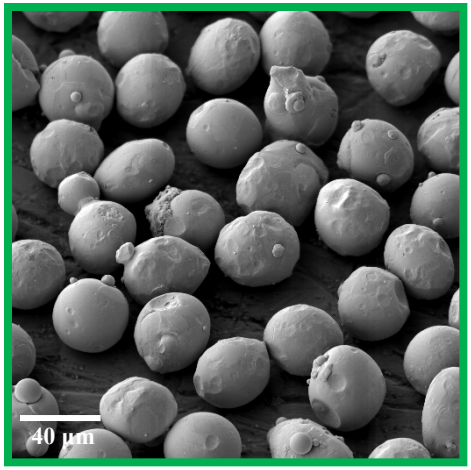

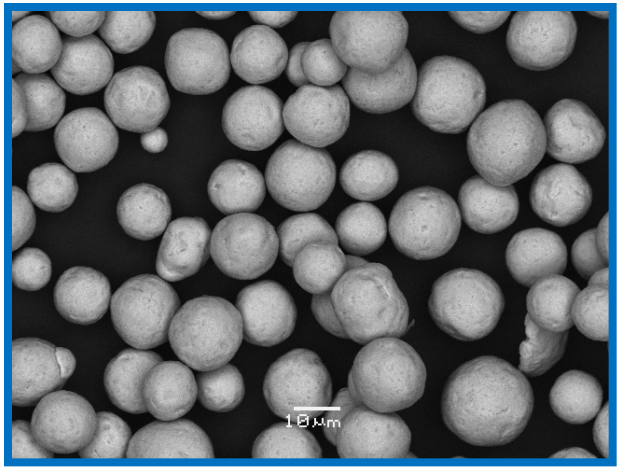

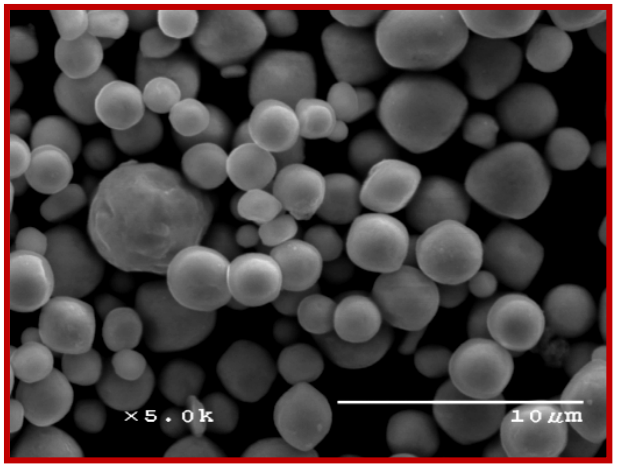

32-38µm | **15-20µm** | **-5µm**

- Auger depth profiles show enrichment of O and Cr at powder surface
- Oxide shell thickness decreases with powder size (cooling rate sensitive)

As-Atomized Microstructure

CR-156Y-Hf: Fe-15.84Cr-0.11Hf-0.18Y-0.38O at.%

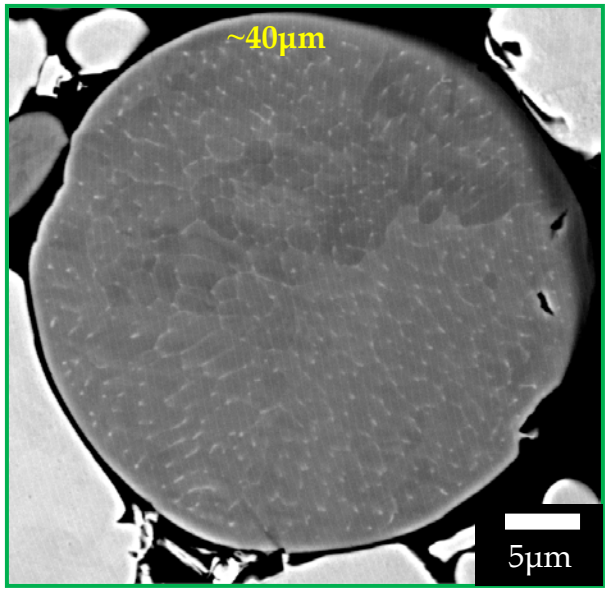

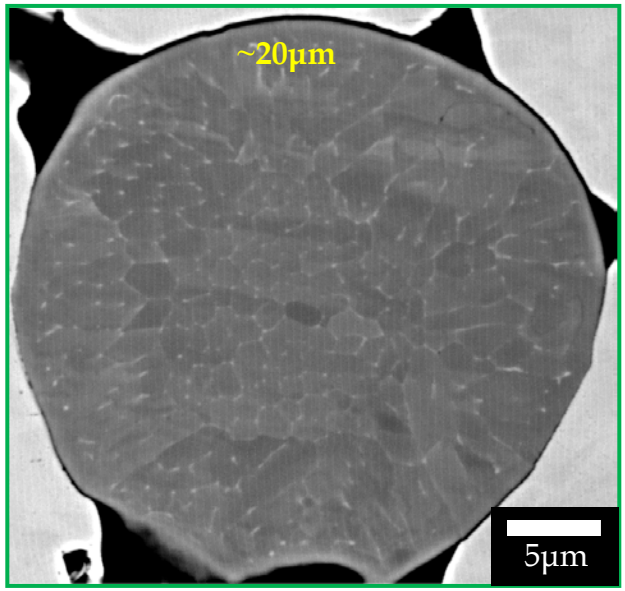

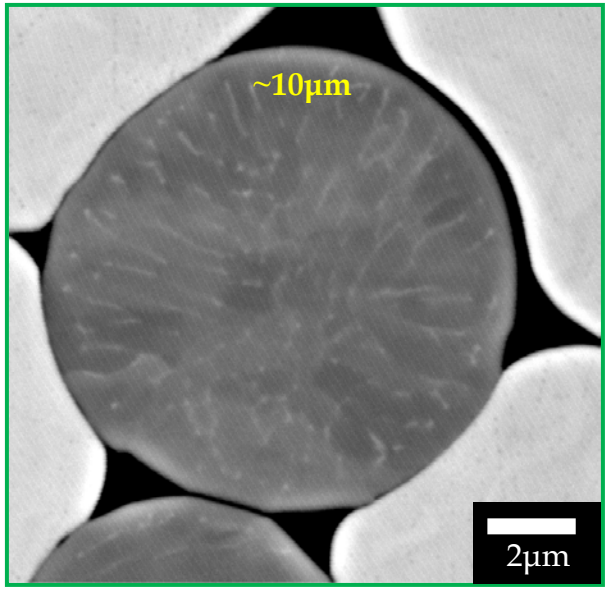

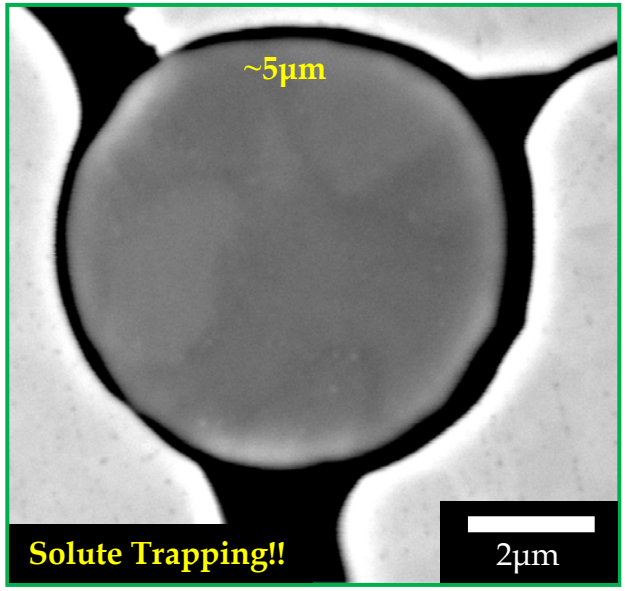

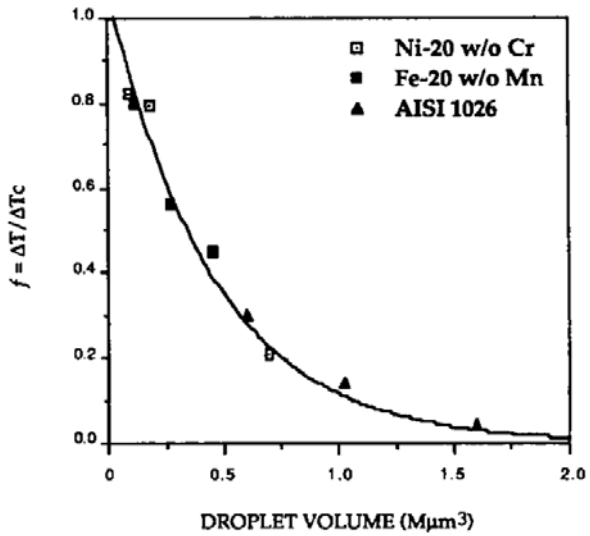

*P. Mathur et al., J. Acta. Metall., 1989. **37**: p.p 429-443

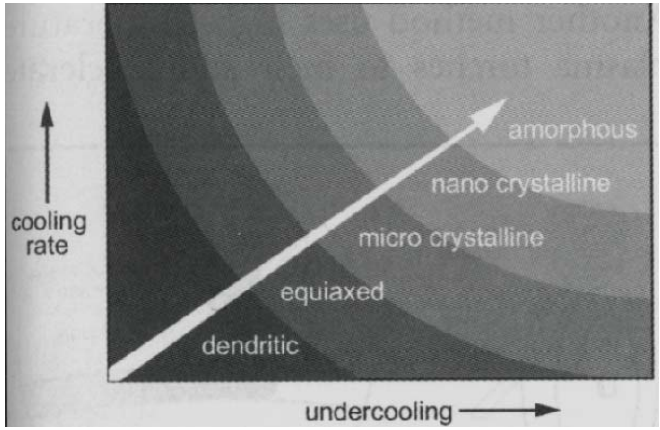

**R.M. German, *Powder Metallurgy and Particulate Materials Processing*, 2005, MPIF, Princeton, NJ.

As-HIPped (700°C) Microstructure

CR-156Y-Hf: Fe-15.84Cr-0.11Hf-0.18Y-0.38O at.%

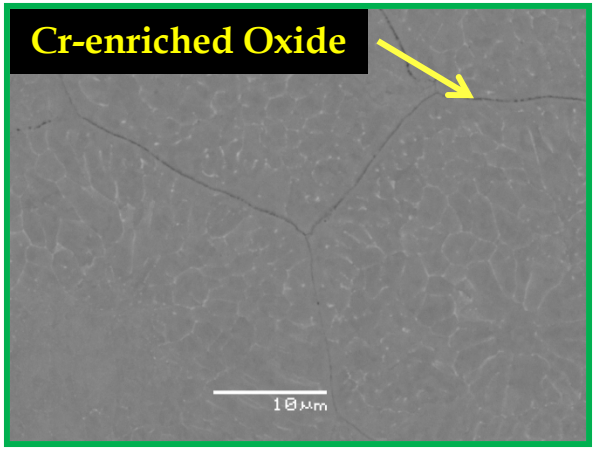

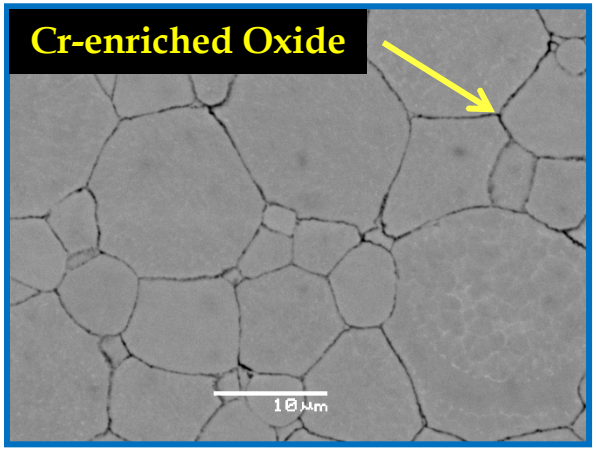

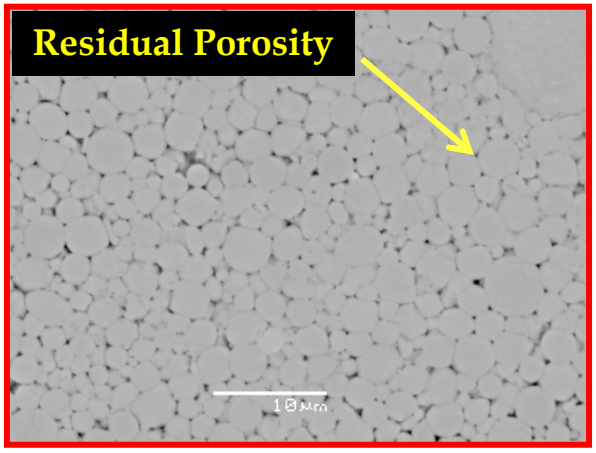

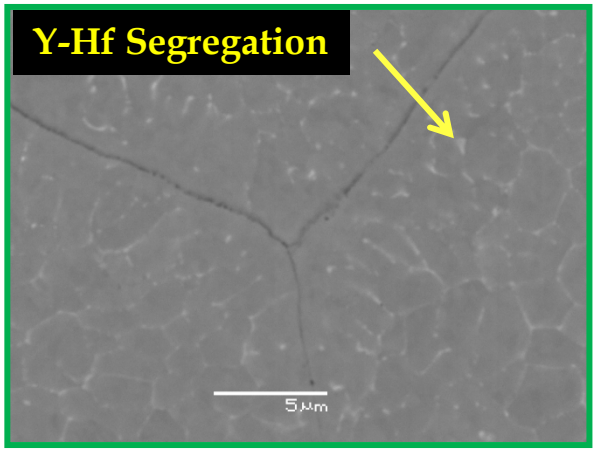

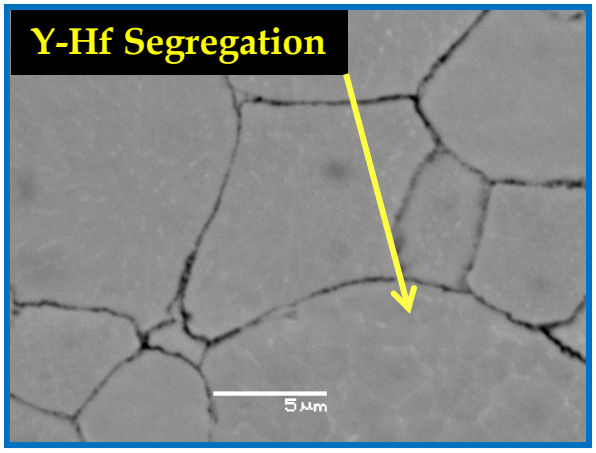

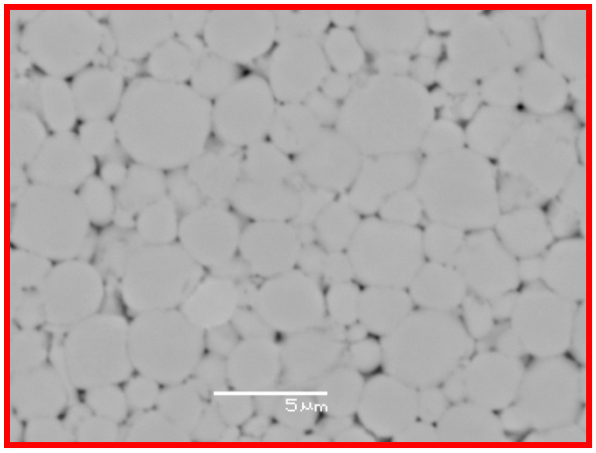

20-53µm	5-20µm	-5µm

As-HIPped (700°C) Microstructure

CR-156Y-Hf: Fe-15.84Cr-0.11Hf-0.18Y-0.38O at.%

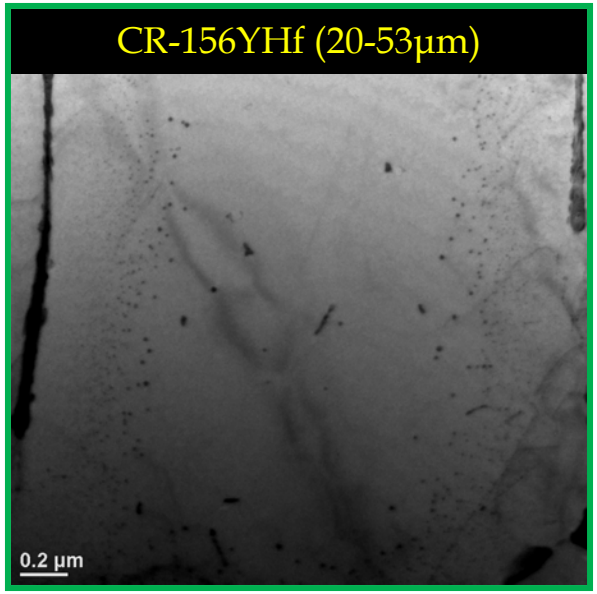

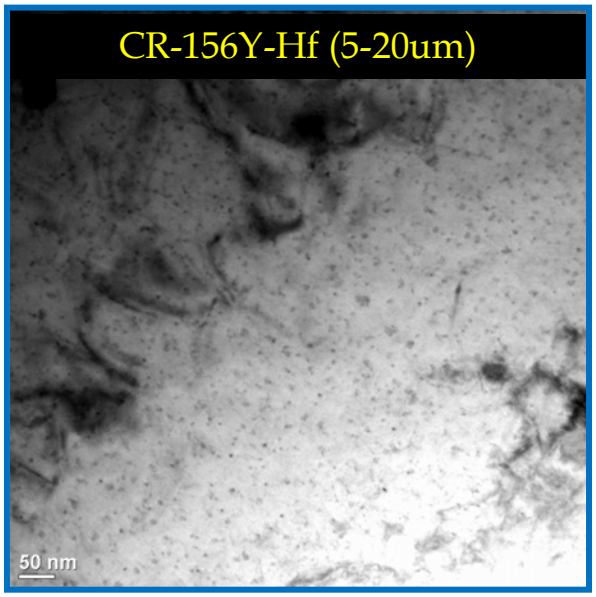

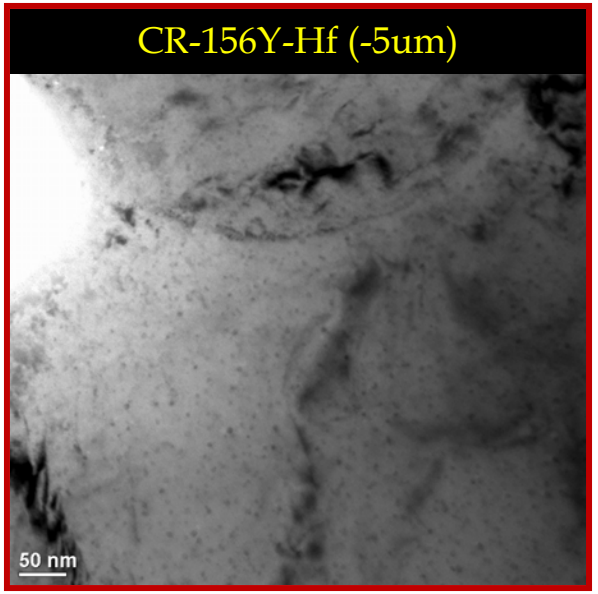

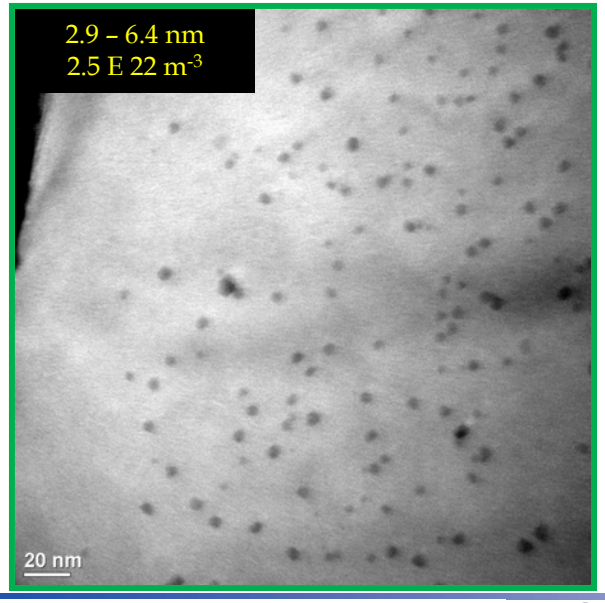

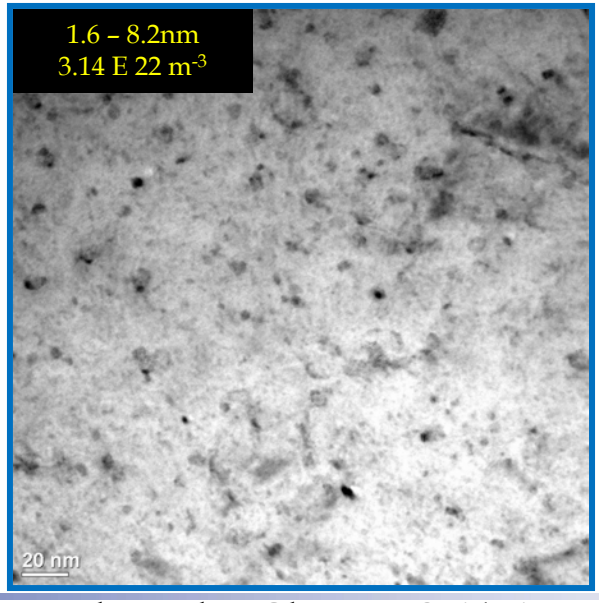

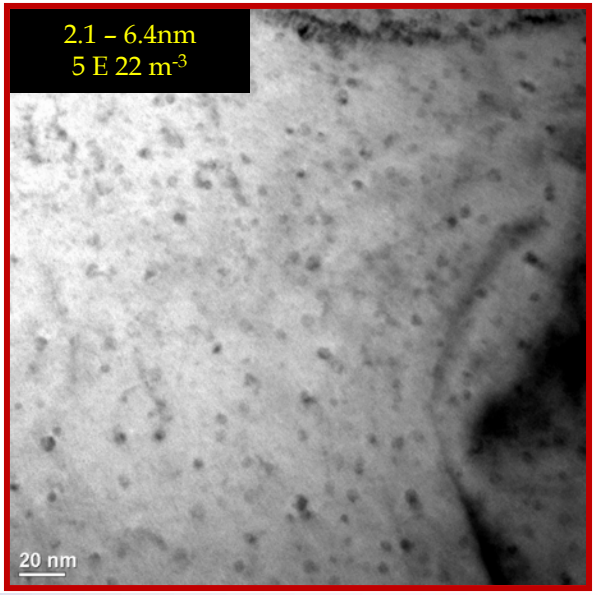

F. Gesmundo, and B. Gleeson, *Oxidation of Metals*, 1995, vol. 44, pp. 211-237.

CR-156Y-Hf: Fe-15.84Cr-0.11Hf-0.18Y-0.38O at.%

Heat Treated 1200°C Microstructure

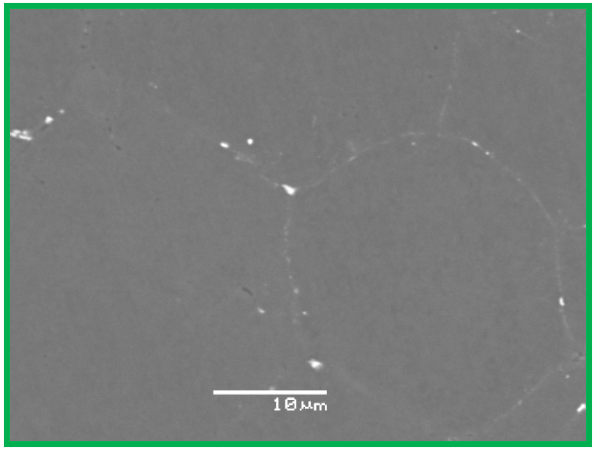

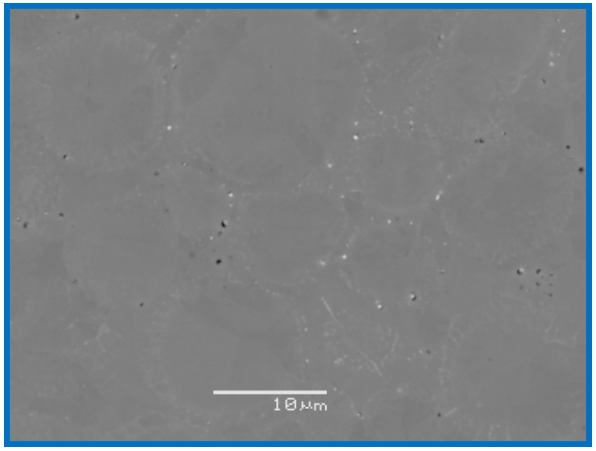

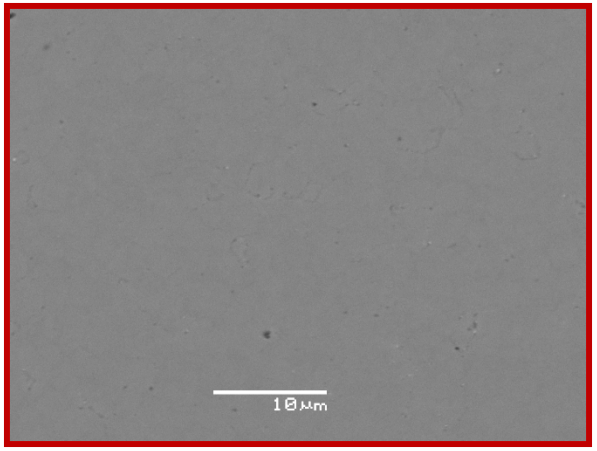

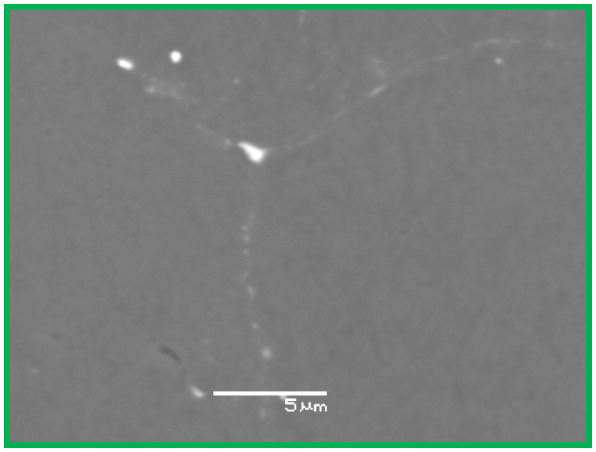

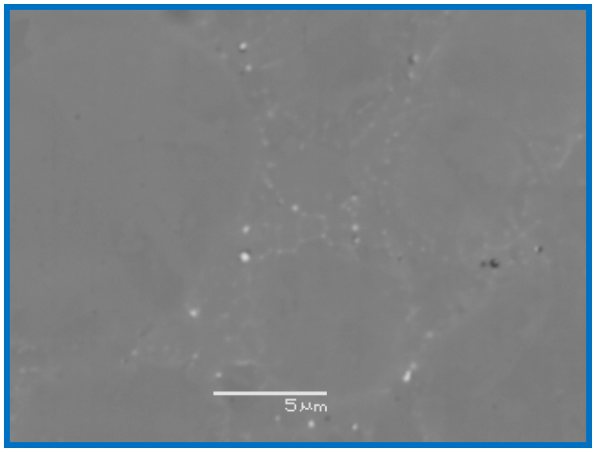

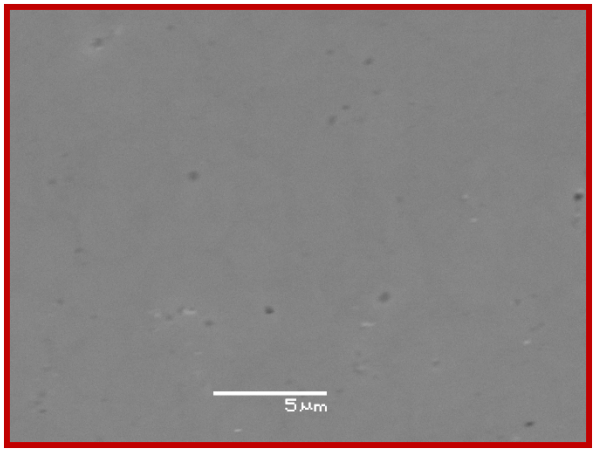

20-53µm	5-20µm	-5µm

Increasing Oxygen Content

Decreasing Residual Intermetallic Precipitates

CR-156Y-Hf: Fe-15.84Cr-0.11Hf-0.18Y-0.38O at.%

Heat Treated 1200°C Microstructure

CR-156YHf (20-53µm)

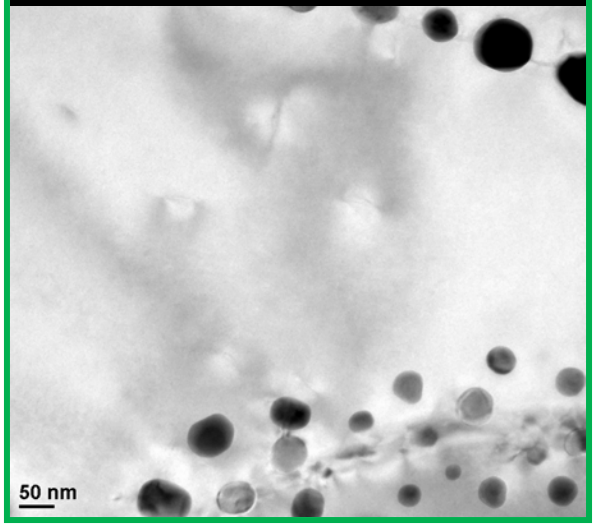

CR-156Y-Hf (5-20um)

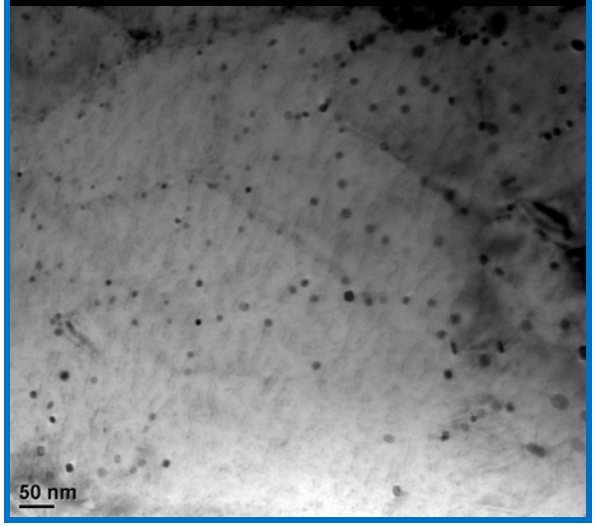

CR-156Y-Hf (-5um)

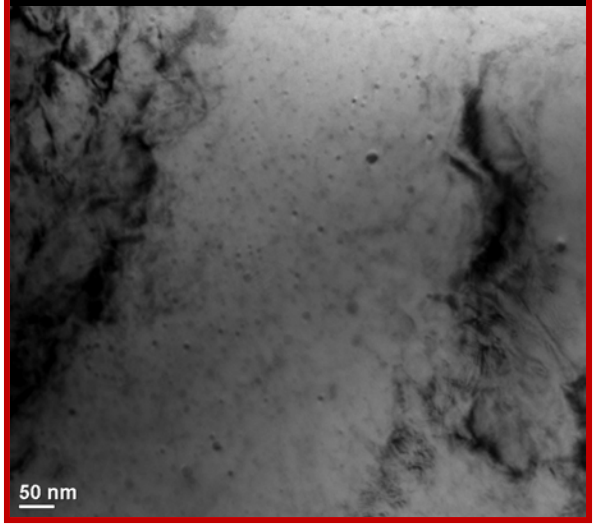

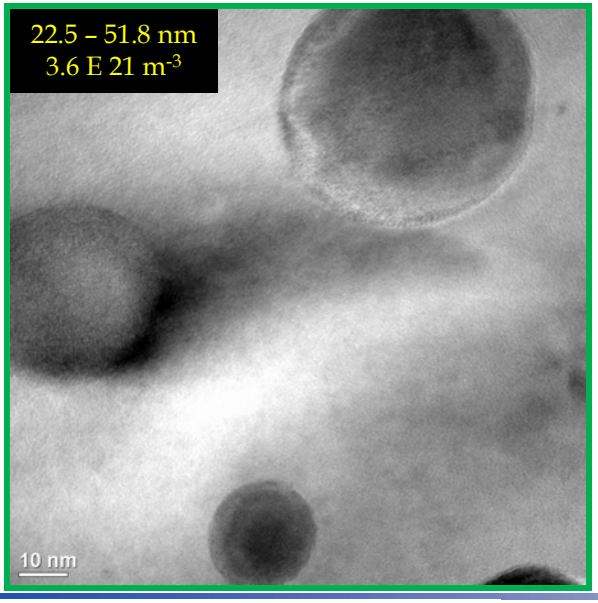

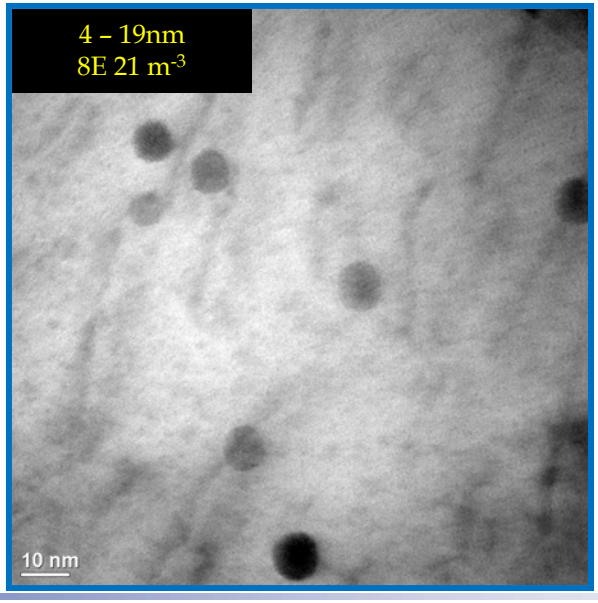

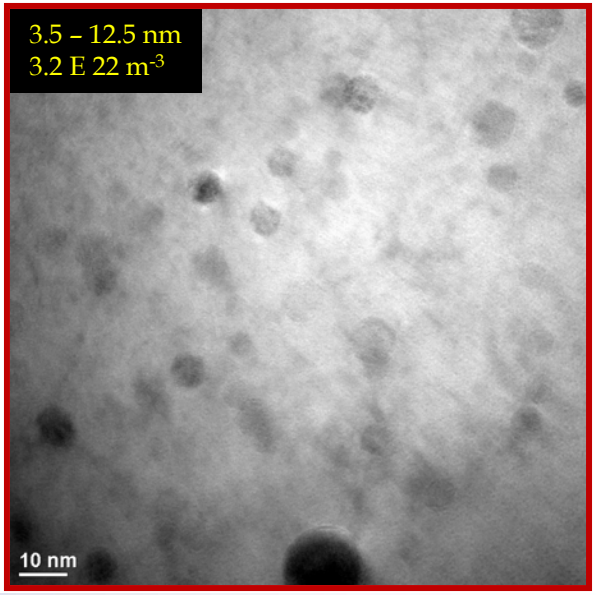

Dislocation Substructure Development

CR-156Y-Hf: Fe-15.84Cr-0.11Hf-0.18Y-0.38O at.%

- Heat Treated Bars
- Cold Rolled
- Annealed (dislocation recovery)

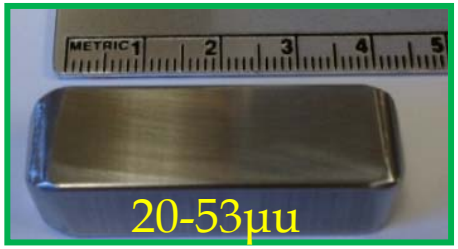

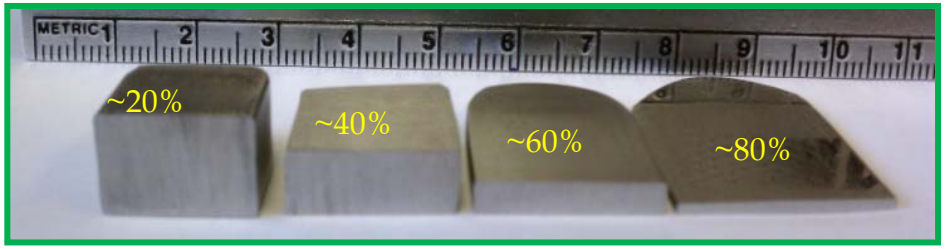

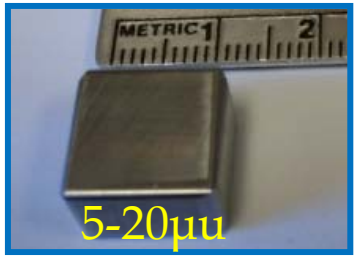

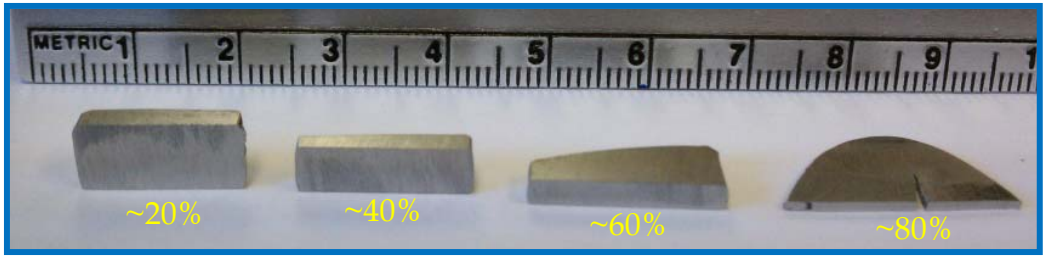

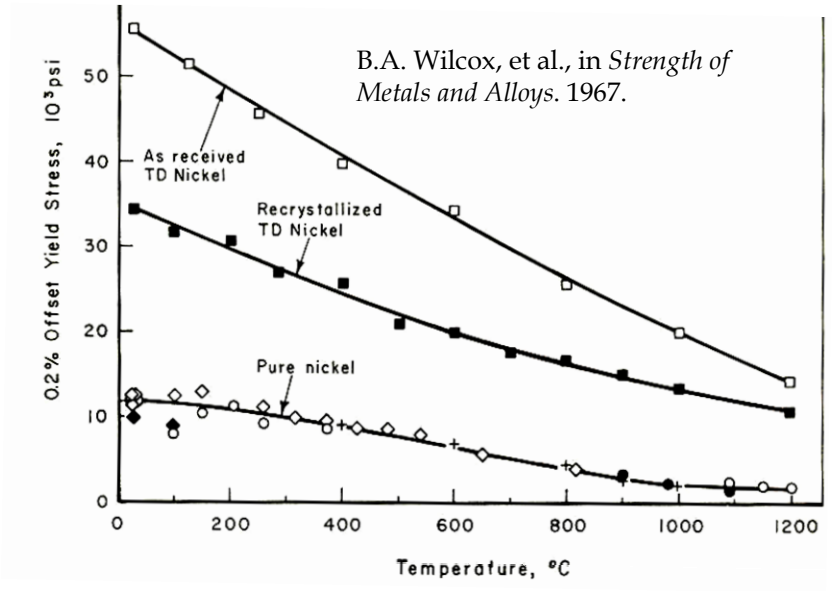

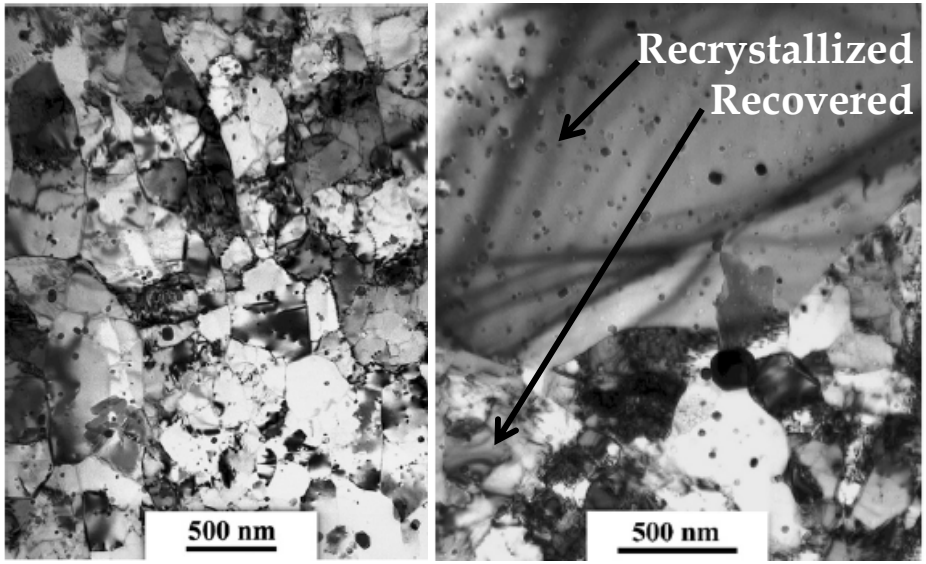

MA-956

M.F. Hupalo, et al., ISIJ Inter., 2004. **44**(11)

Dislocation Substructure Development

CR-156Y-Hf: Fe-15.84Cr-0.11Hf-0.18Y-0.38O at.%

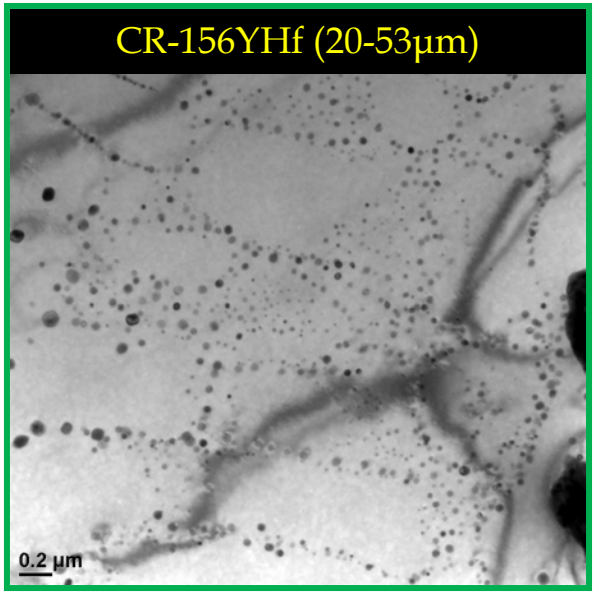

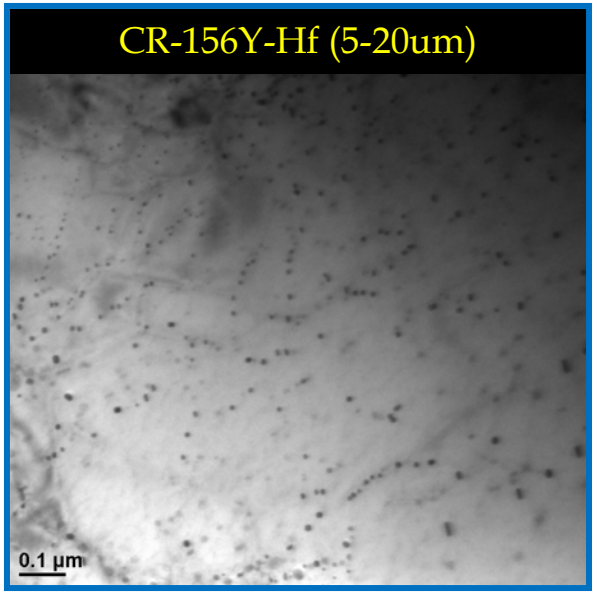

As-Reacted
(Heat Treated 1200°C)

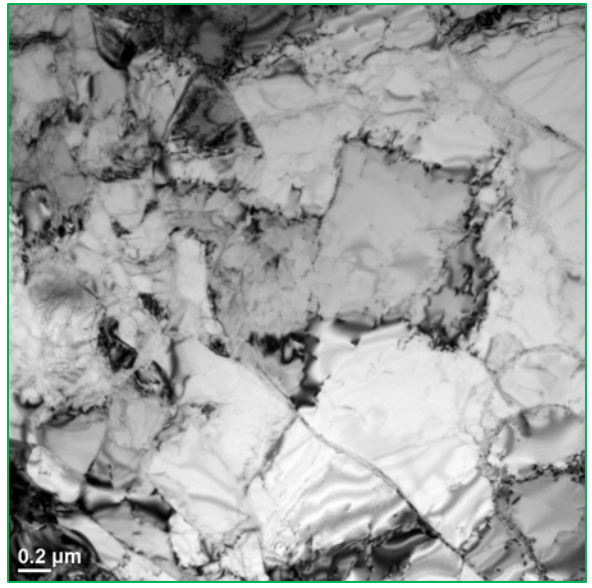

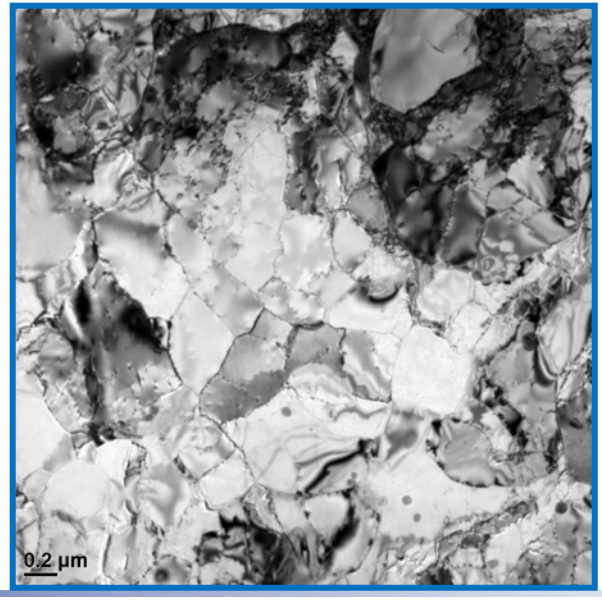

Cold Rolled 80% RA
Annealed 500°C-1hr
(Dislocation Recovery)

Vickers Microhardness Results

CR-156Y-Hf: Fe-15.84Cr-0.11Hf-0.18Y-0.38O at.%

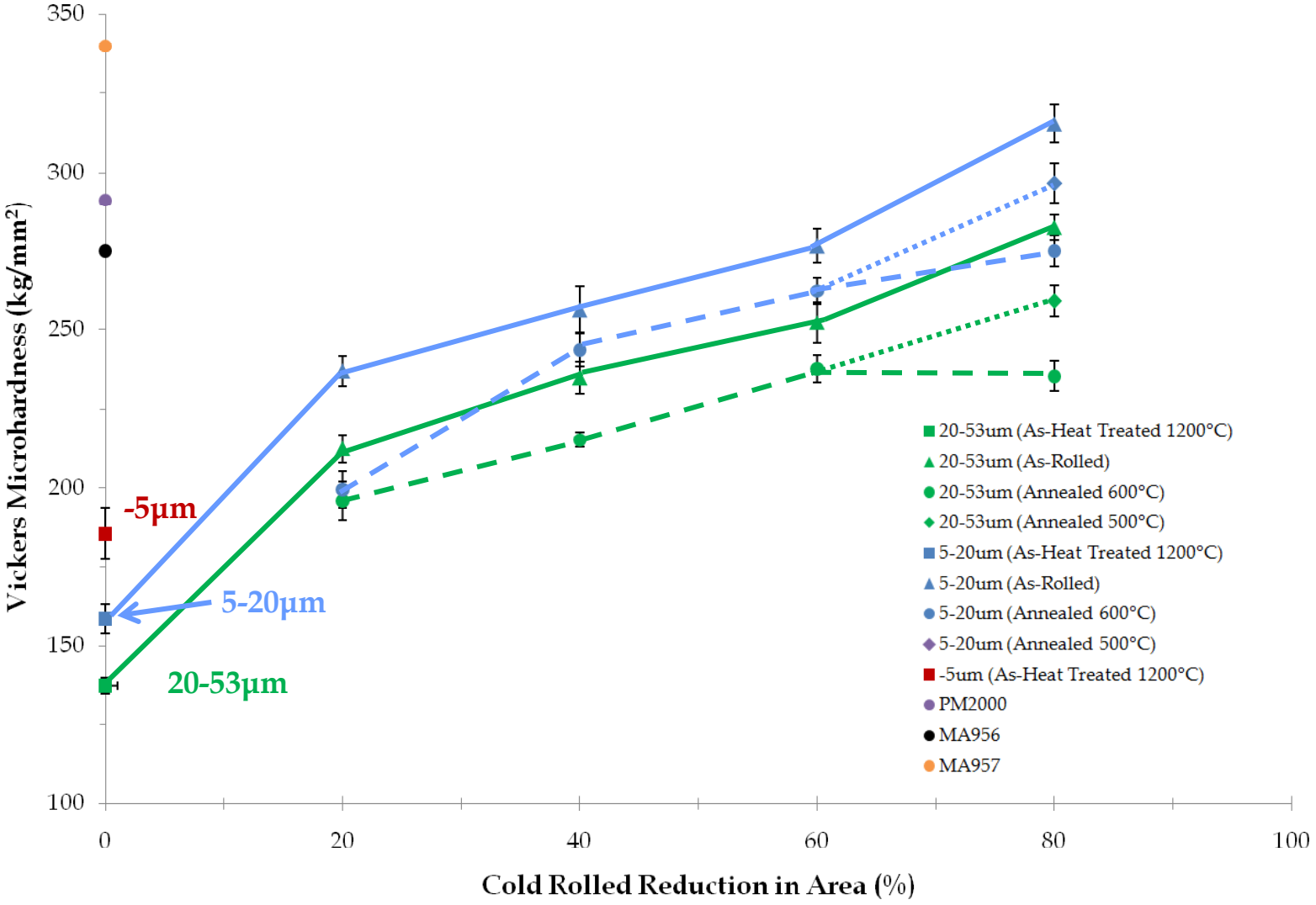

Vickers Microhardness Results

CR-156Y-Hf: Fe-15.84Cr-0.11Hf-0.18Y-0.38O at.%

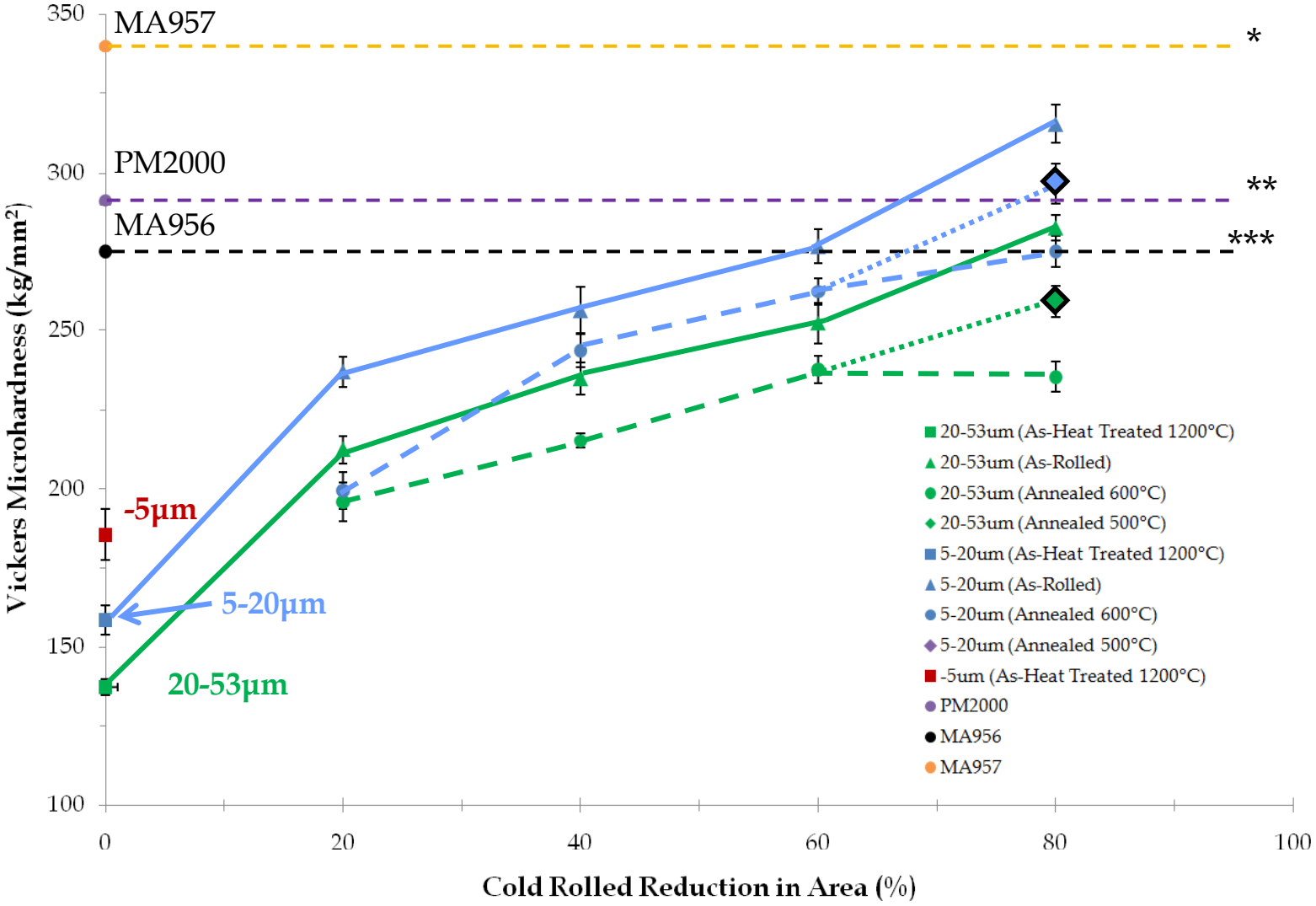

*M.J. Alinger, et al. Fusion Mater. Semiannu. Prog. DOE-ER-0313/43, 2008. **DOE, Oak Ridge, TN**: p. 57-79.

C. Capdevila, et al. Mat. Sci. Eng., 2008. **A 490, pp. 277-288.

***Incoloy® MA956 Material Properties Data Sheet (www.special metals.com)

CR-Alloy Microstructure Summary

- **A new simplified processing* technique involving gas atomization and in situ oxidation has been developed to produce precursor ferritic stainless steel powder that can be consolidated into an oxide dispersion strengthened alloy with an isotropic microstructure.**
- **Resulting oxygen content was successfully predicted using an empirically developed linear processing model, depending inversely on particle size.**
- **Phase analysis confirmed that nano-metric Y-enriched oxide dispersoids formed by oxygen release/transport/reaction during elevated temperature heat treatment.**
- **Resulting ODS microstructures were shown to be highly dependent on powder particle size (i.e., solidification rate). Particles with increased amounts of solute trapping (<20μm) resulted in smaller and more evenly distributed nano-metric oxide dispersoids.**
- **Selection of powder particle size range was shown to be a viable method to control the final ODS microstructure.**
- **Thermal-mechanical processing was used to develop a fine scale dislocation substructure, which resulted in significant increases (~2X) in alloy microhardness, as a preliminary test of ultimate mechanical properties.**

*I.E. Anderson, and (estate of) R.L. Terpstra, "Dispersoid Reinforced Alloy Powder and Method of Making," USPatent No. 7,699,905 B1, April 20, 2010.

Acknowledgments

- *Support from the Department of Energy-Office of Fossil Energy is gratefully acknowledged through Ames Laboratory contract no. DE-AC02-07CH11358.*

David Byrd[1], Jim Anderegg[1], Elliot Fair[2], and Alex Spicher[2]

1US Dept. of Energy Ames Laboratory, Materials and Engineering Physics, Ames, IA 50011

2Iowa State University, Material Science and Engineering (Undergraduate Student), Ames, IA 50011

Close-Coupled Gas Atomization

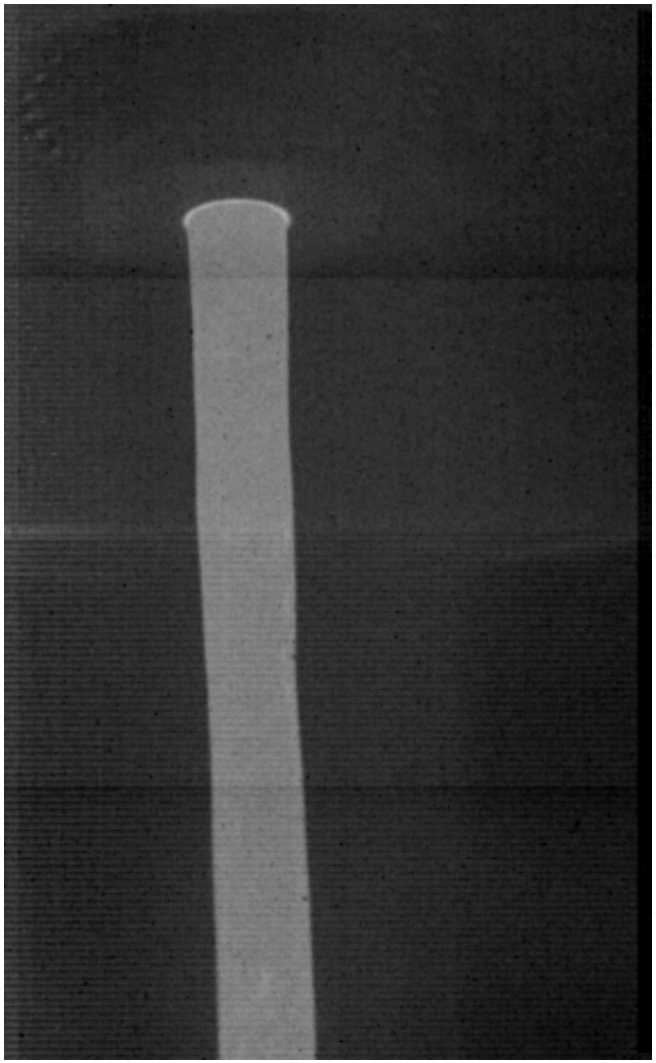

~0.1s real atomization time

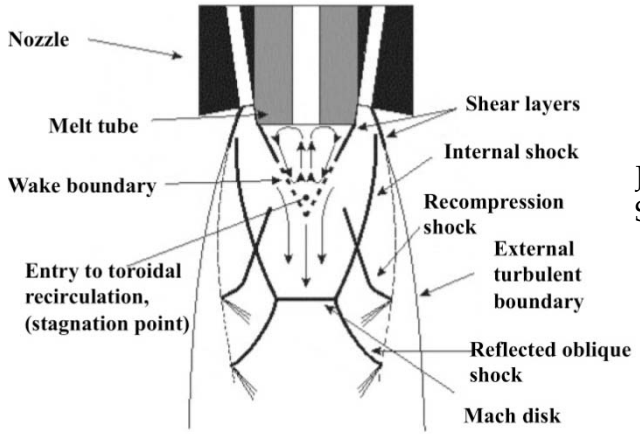

J. Ting and I.E. Anderson, Mat. Sci. Eng., A379 (2004), 264-276.

ACCELERATION / LIGAMENTATION

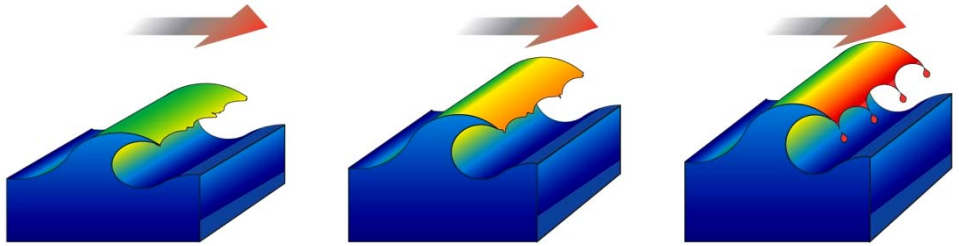

$$D_m = \frac{D_0}{0.027}\left[We_g Re_L\right]^{-0.4}, \text{ for } We_g Re_L > 10^6$$

$$We_g = \frac{\rho_g \Delta U^2 D_0}{\sigma_{LV}} \qquad Re_L = \frac{\rho_L \Delta U\ D_0}{\mu_L}$$

R.D. Ingebo, NASA Technical Paper 1791, National Aeronautics and Space.

Microstructure Evolution(CR-156Y-Hf)

CR-156Y-Hf: Fe-15.84Cr-0.18Y-0.11Hf-0.38O at.%

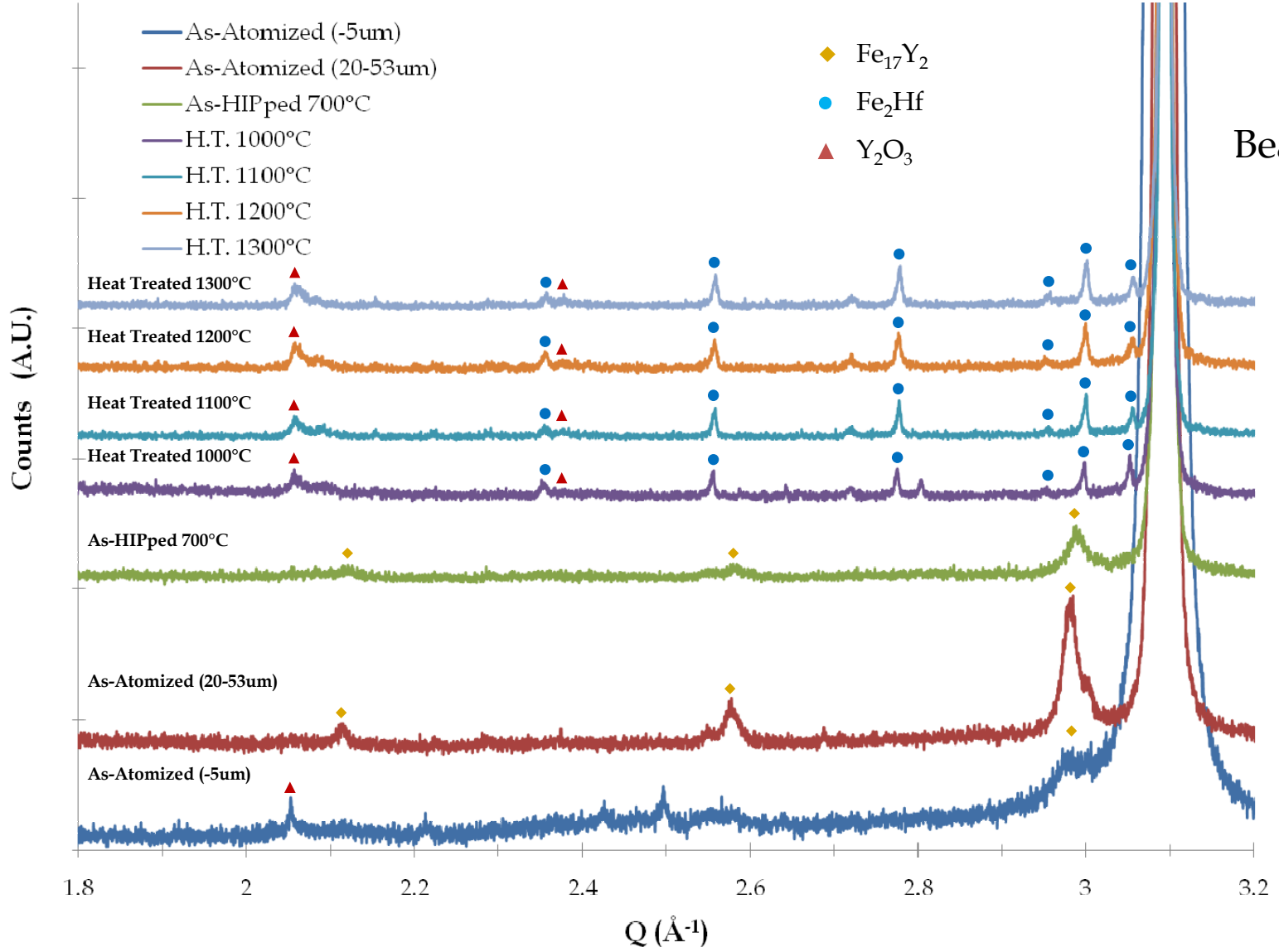

APS Data
HE-XRD
Beamline (11-BM)

The Ames Laboratory
Creating Materials & Energy Solutions
U.S. DEPARTMENT OF ENERGY

The high energy X-ray work at beamline 11-BM of the APS was supported by the Department of Energy, Office of Science, Basic Energy Sciences under contract no. DE-AC02-06CH11357

Iowa State University
of Science and Technology

Microstructure Evolution(CR-156Y-Hf)

CR-156Y-Hf: Fe-15.84Cr-0.18Y-0.11Hf-0.38O at.%

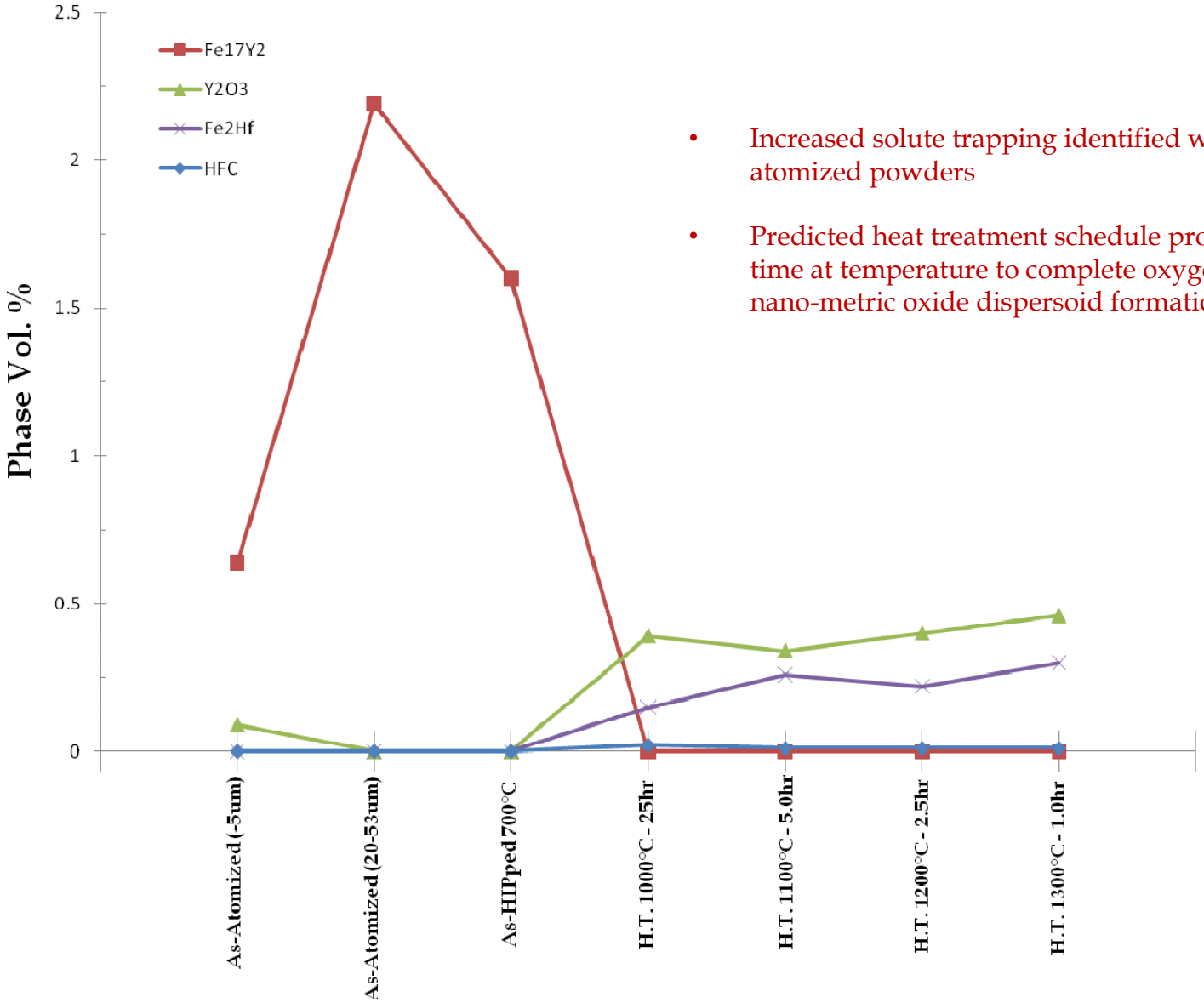

- Increased solute trapping identified within fine (-5μm) as-atomized powders
- Predicted heat treatment schedule provided sufficient reaction time at temperature to complete oxygen exchange reaction (i.e., nano-metric oxide dispersoid formation)

Mechanical Properties of Initial Samples

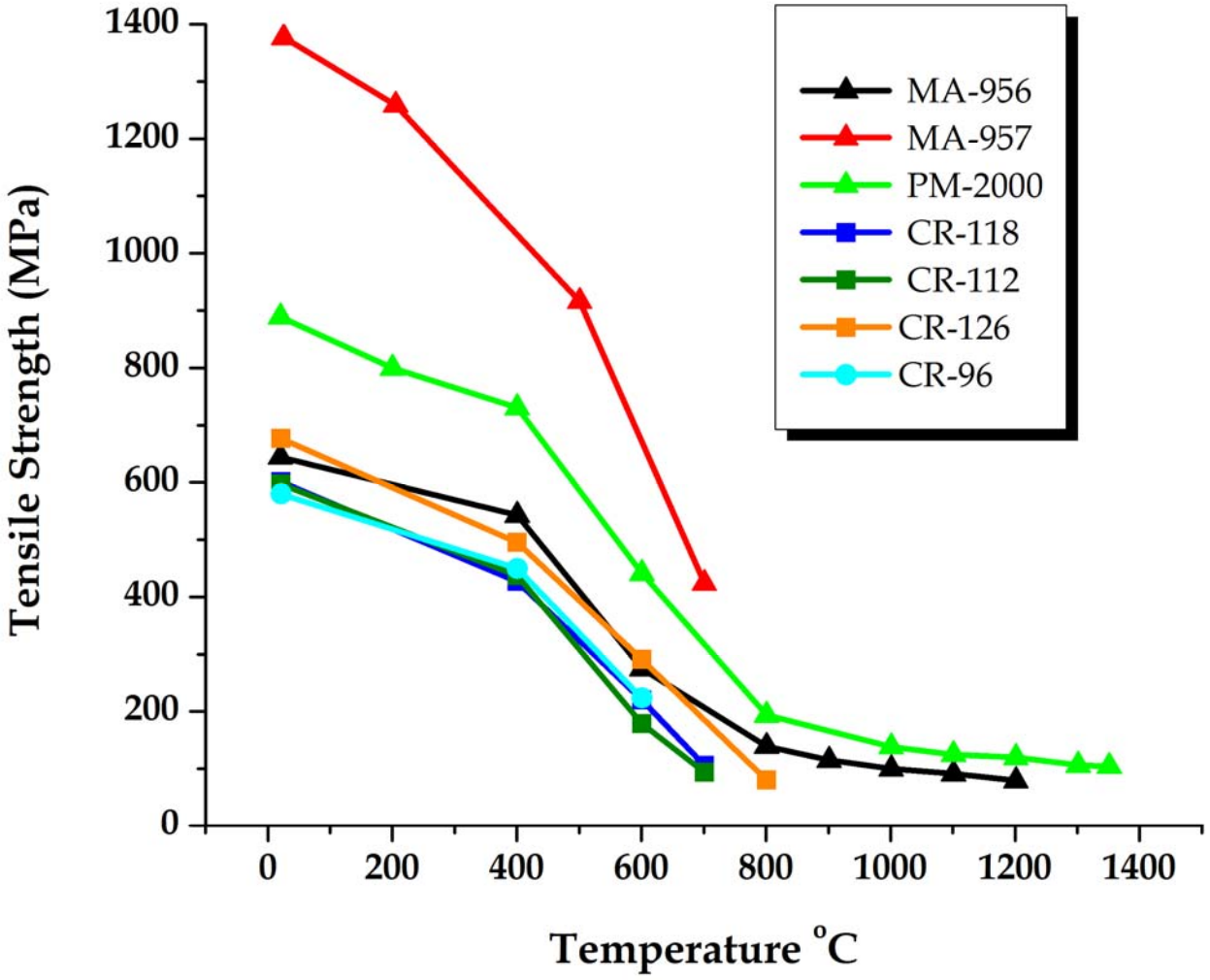

- **As-HIP (1300˚C, 4h) samples of CR-alloys machined to tensile bars.**
- **CR-alloys were tested with a non-ideal microstructure (residual PPB oxide)**
- **Similar tensile strength as MA-956 with approx. three times the total elongation**
- **All commercial alloys converge above 800°C**
- **All CR-Alloys illustrate similar tensile strength due to related isotropic microstructures**

R.L. Klueh, et.al., J. of Nuc. Mat., 2005. **341**: p. 103-114.

Failure Analysis-Microstructure

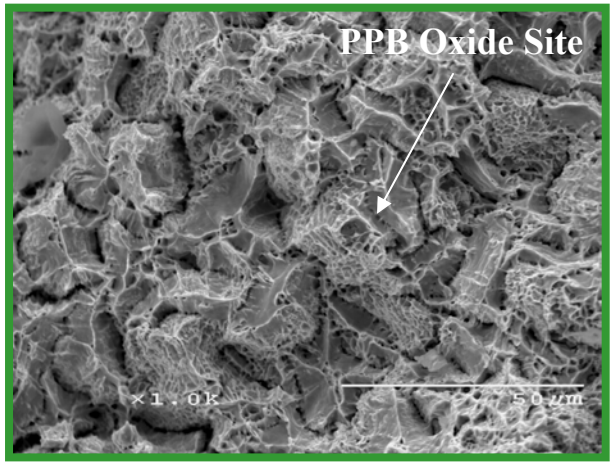

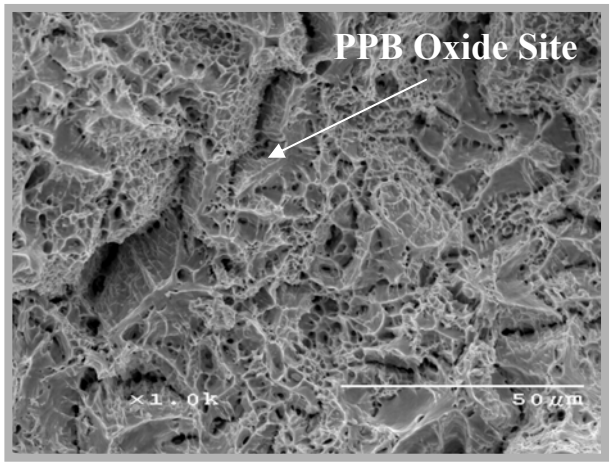

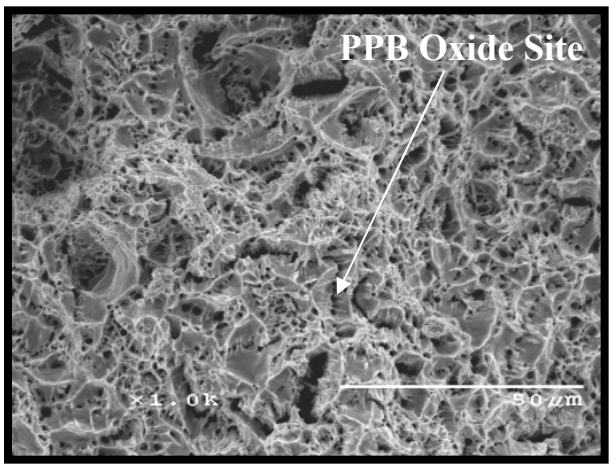

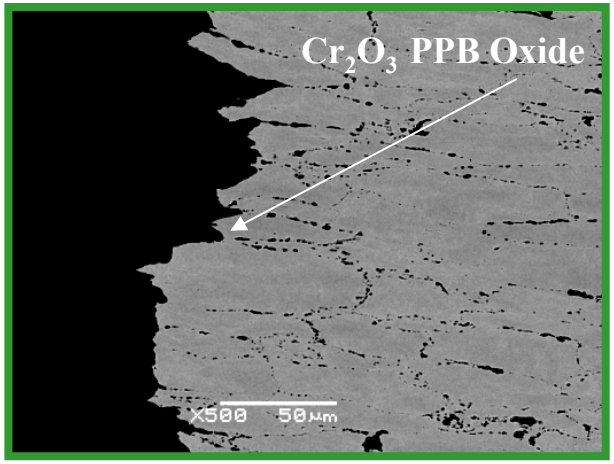

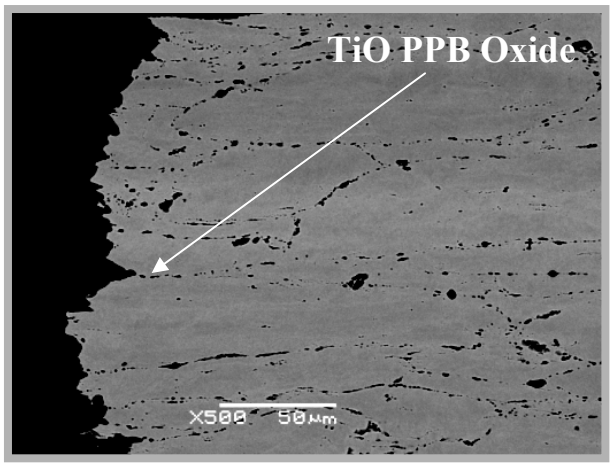

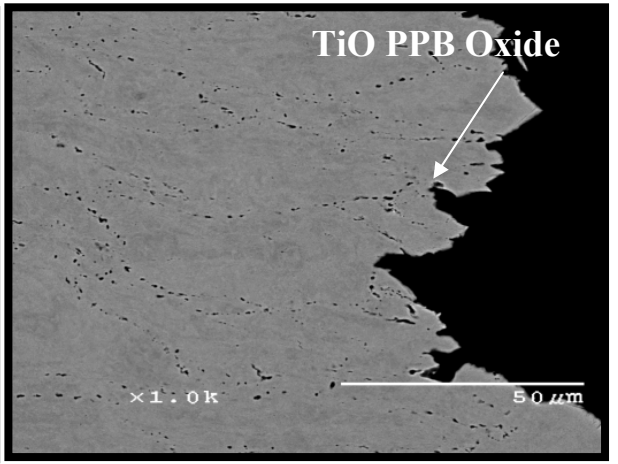

CR-112 CR-118Ti CR-126TiW

Failure occurs by micro-void formation/coalescence resulting from the debonding of the matrix from residual non-ideal phases (i.e. PPB oxide)

Failure Analysis (Fracture Surface)

CR-96 (1st)

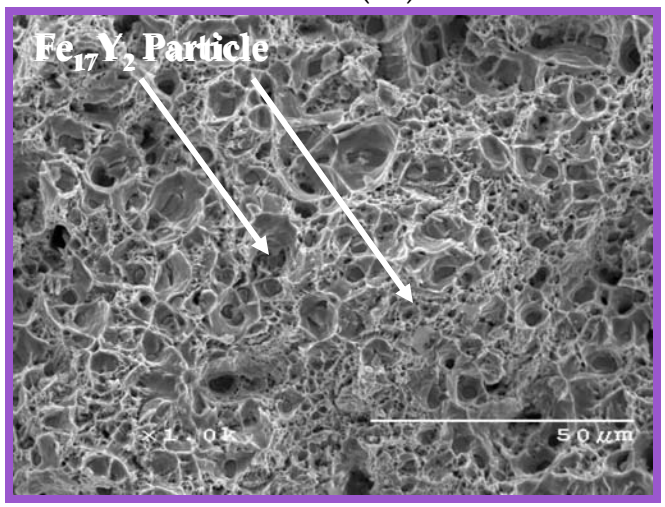

CR-112 (2nd)

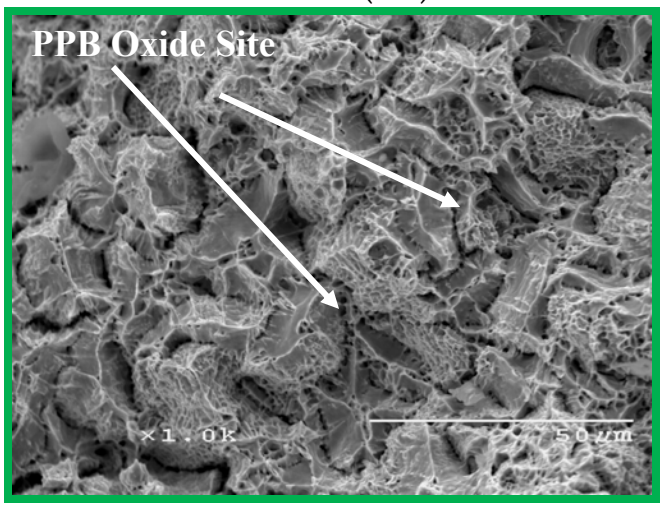

CR-118+Ti

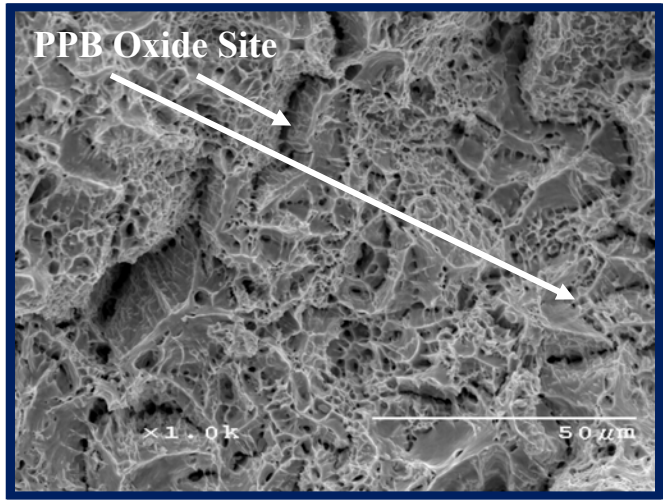

CR-126+TiW

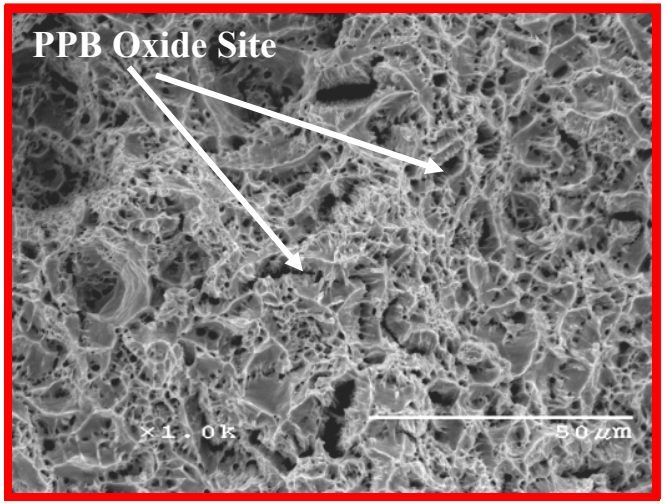

Failure Analysis (Fracture Cross-Section)

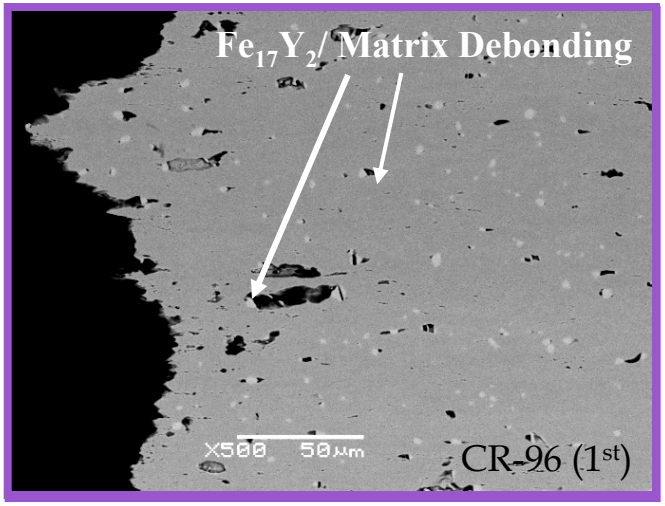

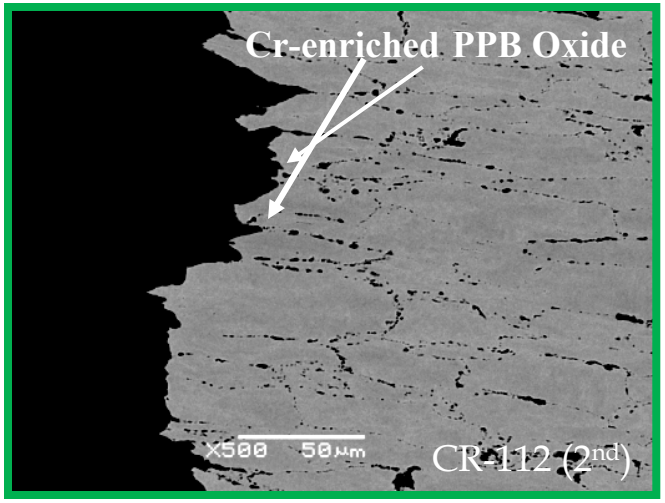

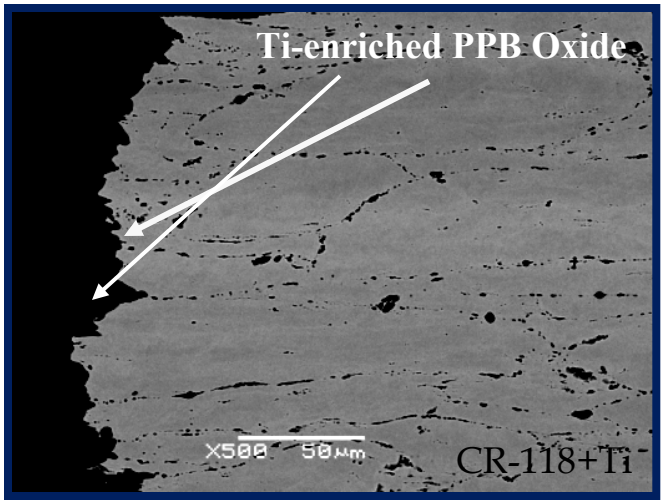

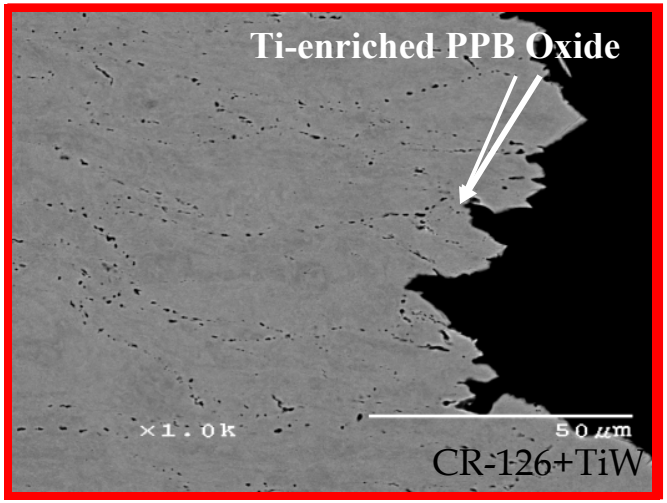

Failure occurs from micro void formation resulting from the debonding of the matrix from residual non-ideal phases (i.e., PPB oxide)